

The paper tackles the problem of climate change in the Mediterranean, exploring the role of teleconnections and local feedbacks in modulating future projections. To this aim, climate simulations are designed and run using a state-of-the-art climate model. The authors find climate change in agreement with previous literature (warming and drying), however their findings suggest reduced amplitudes in change. They explain these differences with the improved ability of the model in simulating SNAO teleconnections and land surface feedbacks.

**We thank the reviewer for their very thorough revision comments and feedback regarding our manuscript. We have addressed all of the major comments when revising the manuscript. This includes either applying the reviewer's suggestion or a thorough justification for not doing that. We have also made an effort to address the minor comments. Overall, we have substantially reworked the text of the manuscript to improve its conciseness and clarity. The manuscript is shortened by ~20%. The main focus of the study, described in the Introduction, is clarified. The key messages of the study, presented in the Discussion and Summary section, are clarified and enhanced. The number of figures is reduced from 12 to 10, by merging Figure 1 and 2 (in the previous version) into Figure 1, and Figure 8 and 9 (in the previous version) into Figure 6. We have also reworked the structure of the manuscript, so the text discussing the results is now included in Discussion and Summary. We have clarified the abstract.**

**We have also removed the discussion of the North Atlantic storm track, and the relevant figure (Figure 7 in the previous version of the manuscript). This part of the discussion will be very important in the further study that investigates the impact of the SNAO on northern Europe, but it is of minor importance for the Mediterranean hydroclimate investigated in the current manuscript.**

Major comments 1. I acknowledge the huge work the authors did in carefully revising and discussing the literature, and in performing and discussing many analysis, but this makes the paper very long. My first general recommendation is to somehow shorten the manuscript, to facilitate the reader to be focused on the key messages delivered by the paper. For instance, discussions of previous findings is sometimes too detailed and redundant: accepted knowledge on summer climate in the Mediterranean region should be described in detail in the Introduction (or in a dedicated Background section) and briefly recalled when necessary in the text.

**AU: Thank you for the comment. Following the reviewer's suggestion we have reworked the manuscript to make it more comprehensible. The discussion of the previous studies is summarized in a more concise way and moved to the Introduction or to the Discussion and Summary section. The accepted knowledge on the regional summer climate is moved from the section 3.2.1. and 3.2.2 (in the previous version: pp 9: lines 1-46, pp 10: lines 7-21) to the Introduction (in the current version: pp1, l 45 – pp2, l 29; pp2, l 40- pp3, l 18). Please note that the Introduction is partly rewritten and shortened. The results are discussed through the prism of previous findings, and those are recalled when necessary in Discussion and Summary (in the current version: pp 15, l1-15, pp 16 l 25-46). The Discussion and Summary is substantially rewritten and shortened, the key message is highlighted and clarified.**

2. The main finding of the paper is the different amplitude of future projection of the Mediterranean climate simulated by the CM2.5 model in comparison with CMIP3 and CMIP5 simulations. To illustrate this crucial aspect, the authors refer to the existing literature on the topic. However, when quantitative differences are discussed, comparison with a Figure would be helpful. I suggest the authors to add some figures (in the supplement) showing projections of the future Mediterranean climate (precipitation and temperature) in the CMIP5 ensemble or, if downloading CMIP5 data is too time consuming, at least the CM2.1 model output, to show differences with the same model at lower resolution and not including the improved land model LM3.

**AU: Thank you for the suggestion. In order to facilitate the comparison between the CM2.5 future projections and other models we have updated references and also included a supplementary figure. Figure R1 depicts changes estimated based on the RCP8.5 CSIRO-Mk3-6-0 model 10-member projections ensemble. Unfortunately, there are no RCP scenarios for GFDL CM2.1. Instead, we use**

the CSIRO-Mk3-6-0 model, which includes the ocean component based on the GFDL ocean model. We also refer to the very comprehensive analysis in Jacob et al. 2014 and Fussler et al. 2017 (Map 3.4, pp. 76), employing many GCM-RCM combined simulations from the EURO-CORDEX project. Discussion of these results is included in the text (pp10: lines 34-41, pp 16: lines 25-32).

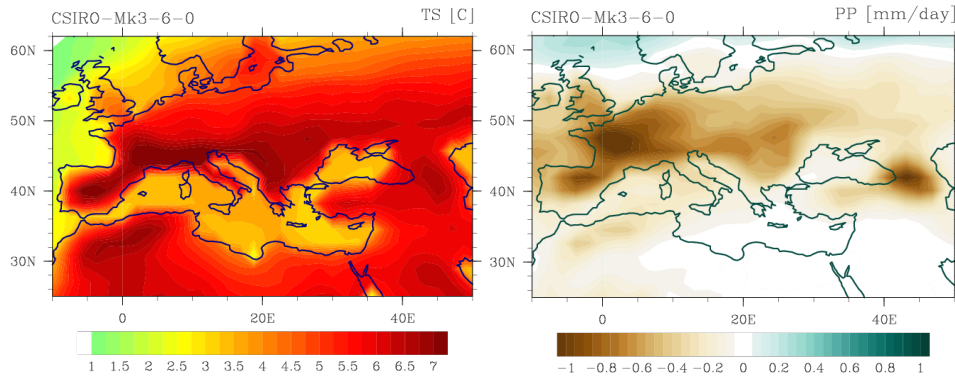


Figure R1. Projected future changes for the summer (JJA) surface temperature (left, °C), and precipitation (mm/day, right) based on the 10-member ensemble simulations of the CSIRO-Mk3-6-0 model, for the forcing scenario RCP8.5.

3. Data: why NCEP reanalysis are selected for comparison? On the same period, ERAI data are available at higher resolution. ECMWF datasets are also available for the 20th century. Same question about precipitation data: why University of Delaware? Testing other temperature/precipitation datasets (CRU, EOBS) would change your results? In general, comparing your results with different datasets would improve the robustness of your conclusions.

**AU:** Yes, we agree that a verification of the results with different datasets would improve the robustness of the conclusions. Following reviewer’s suggestion we have incorporated EOBS dataset in the analysis of the regional precipitation (Figure 3). We agree that EOBS provides high quality data and serves as a good reference for the regional precipitation. Given the same spatial resolution as CM2.5, EOBS allows for comparing very fine features over the complex orography of the Mediterranean.

However, incorporating datasets with higher resolution would not necessarily serve the purpose of the analysis of the large-scale circulation features. We have included below an additional figure (Figure R2), depicting sea level pressure and wind vector at 850hPa both in ERA-I and ERA 20CR, showing very good agreement between the suggested observational datasets.

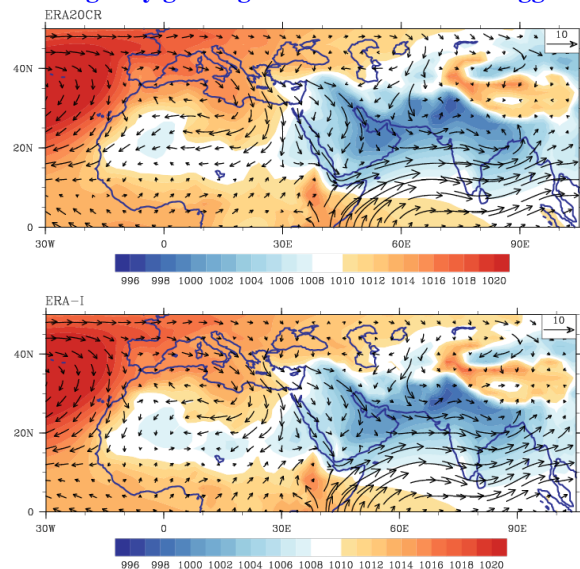


Figure R2. Seasonal (JJA) sea level pressure (hPa) and wind vector at 850hPa (m/s) in (top) ERA-20C, (bottom) ERA-I; for the 1979-2017 period.

**In the analysis of the mid-level and upper level atmospheric dynamics, we would refrain from using the 20<sup>th</sup> century data sets such as ECMWF's ERA-20C or NOAA-CIRES 20<sup>th</sup> Century Reanalysis. Both of these data sets are based on the assimilation of the surface pressure values, which makes them a less plausible reference in the analysis of the upper level atmospheric dynamics. For example, the comparison of the vertical velocity at 500 hPa in Figure R3 reveals a strong positive bias in ERA-I, compared to the rest of the analyzed datasets (note the difference in the scalebar).**

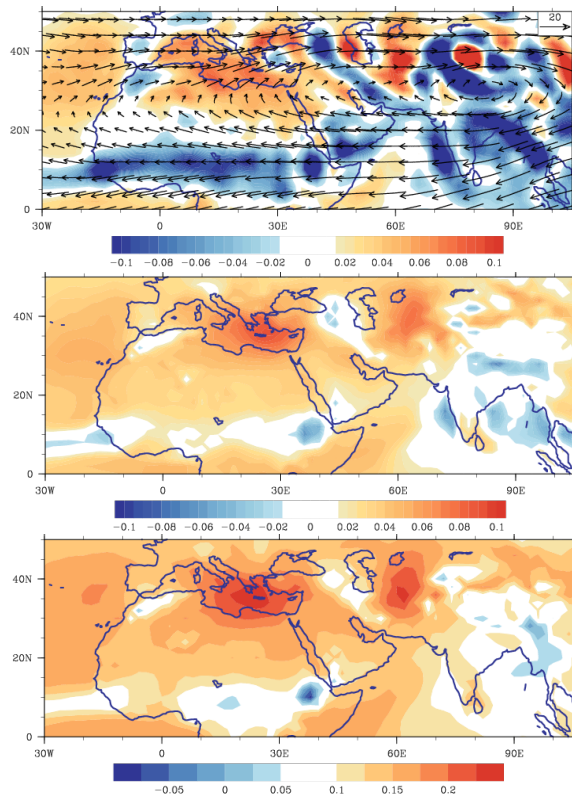


Figure R3. Seasonal (July) time-mean vertical velocities at 500hPa (Pa/s), estimated for (top) NOAA-CIRES 20th Century Reanalysis, (middle) as ECMWF's ERA-20C, (bottom) ERA-Interim for 1979-2017.

4. One main issue of the paper is the choice of the time window to be analysed. The aim of the paper is to study summer Mediterranean climate, so that you select JJA. However, through the paper, different periods are selected for different analysis: JA or just July. I recommend to homogenize the period to be analyzed (preferably JJA), for better comparison of the results. If there are specific reasons to analyze different period, these reasons should be highlighted.

**AU: The choice of the time window is dictated by the method being most adequate to the analyzed climate component.. The teleconnection of SNAO with the climate over the Mediterranean region is manifest mostly during the peak summer, i.e. July-August. On the other hand the analysis in section 3.3. “Summer climate regime over the eastern Mediterranean” focuses on the month of July. “The choice is driven by the fact that the magnitude of subsidence and the Etesians is at its maximum in July while the response of the Rossby waves to monsoon rainfall is also the strongest (Tyrlis et al. 2012, Lin et al. 2007, Lin et al. 2009). The justifications of all the time window choices are included in the manuscript, but we have highlighted this information both in Methods (pp 5, lines: 8-12, 14-17,41-44) and in the text (pp 9, lines: 6-9).**

5. Methods section is rather long and sometimes confused: EOF analysis is described twice, the description of correlation/regression analysis is not really necessary here, as well as the reference to figures discussed later in the paper. I recommend to focus the section on the description of more sophisticated methods, such as EOF and stormtrack definition, and leave the description of correlation/regression analysis to the Results section. The section should be then shortened and optimised.

**AU: We have clarified and rewritten the Method section in a more concise way (pp 6, lines: 12-27, 29-38; pp 7, lines: 1-21). Additionally, we have removed the description of storm track definition (p5, 40-46), which follows the decision of not including the discussion of the impacts of SNAO through the perspective of the North Atlantic storm track.**

6. Model validation: in Figures 1-4 you compare the CTRL simulation to the NCEP data, and I see some important biases in terms of intensity (SLP in monsoonal regions) and location of some features (axes of the anticyclonic circulations at 500 hPa). This is due to the fact that in NCEP reanalysis there is GHG forcing, which is not included in the CTRL simulation (as you also highlight in the text, P21, L34-37). It would not be more consistent to compare the CTRL simulation to a different period, i.e. a period of 20C reanalysis/precipitation less affected by GHG forcing?

**AU: We would refrain from the suggestion offered by the reviewer. Comparing CTRL simulation with a different or longer period of observations than the recent three decades would be a more appropriate solution, from the perspective of contributing forcing components. However, the quality of the observations-based precipitation datasets is much lower before the satellite era (~1979). For the analysis of atmospheric circulation we prefer to use a shorter period of NCEP/NCAR2 (DOE) data set rather than the longer Twentieth Century Reanalysis. We justify this choice with the findings in Krueger et al. 2013. This study has shown that the early part of the SLP record (first half of the 20<sup>th</sup> century) in the Twentieth Century Reanalysis suffers substantial inhomogeneities, most likely associated with the increasing number of observations and improved measurement techniques. Moreover, taking into account that both the NOAA's 20CR Reanalysis as well as ECMWF's ERA-20C datasets assimilate only surface pressure reports, sea ice, and sea surface temperature distributions, the expression of the high level atmospheric variables is highly uncertain in these datasets, as shown for example in the Figure R2 (omega at 500hPa) in the response to question #3.**

7. SNAO simulation: the analysis of SNAO impact in Figure 5 is not compared with any reanalysis product. The SNAO impact on climate in Europe is explained with variations in the stormtrack (Figure 7): why reanalysis data are shown and not model simulation?

**AU: The representation of the SNAO in observations, using the SLP in different time periods, is shown in Figure 6. However the observed impact of SNAO has been shown in detail in Folland et al. 2009 and Blade et al. 2012. We prefer to make a reference to the existing literature rather than to repeat an existing analysis, especially to maintain brevity given major comment 1 requesting that we shorten the manuscript length.**

**Yes, the SNAO teleconnection with hydroclimate in northwestern Europe can be directly explained with variations in large-scale circulation over the North Atlantic and associated variations in storm tracks (as shown in observations and simulations in Folland et al. 2009). In this manuscript we do not intend to investigate the simulated impacts of SNAO on the North-Atlantic storm tracks and the northwestern Europe hydroclimate. This topic will be investigated in a further study. We have clarified the text (pp8, lines: 37-41) and also the main focus of the study (in Introduction, pp3, lines: 20-37). To maintain brevity, given major comment 1 requesting that we shorten the manuscript length, we have removed the figure representing the variations in storm track.**



8. Figure 11: the caption of the figure and discussion at P17 should be improved. You first state that you compute EOFs for the CNTR simulation, than you project the HIST-PROJ fields onto the CTRL EOF to get the 1860-2100 time series. Than you state that you also compute EOFs separately for HIST and PROJ. Then you discuss the 1860-2100 time series in Fig. 11c, then you go to HIST and PROJ EOFs in Fig. 11ab, and finally you discuss the contribution of the 1860-2100 SNAO to the end-of century projection of precipitation (Fig. 11de). I find this discussion confusing. This is a crucial point of the paper and should be presented clearly. I recommend the authors to improve the readability of this section. Moreover, the discussion of the SNAO impact on temperature projection should be significantly expanded.

**AU: In this section we address three problems, which requires three different analysis approaches. We consider important to justify each of them. We have made a substantial effort to optimize the length of the discussion, clarified the discussion and improved the relevant caption (pp 15, 16). Following the reviewer's suggestion, we have clarified this part of the results (p11, lines: 9-39), as well as the caption of the relevant figure and the corresponding methods.**

**Section 3.2.2 investigates the impact of SNAO on the Mediterranean precipitation and temperature, with focus on the former; section 4.2. analyzes the impact of the SNAO from the perspective of climate change. There is very limited knowledge on the impacts of SNAO on temperature (basically two papers: Blade et al. 2012, Folland et al. 2009), and these results are far from unequivocal. The results shown in these two articles differ depending on chosen length of dataset and method of analysis (e.g. whether the correlations are based on interannual variations or including multidecadal signal). Our analysis seems more consistent with Folland et al. 2009, who applied rigorous statistics to avoid effects of autocorrelation caused by low-frequency components in a relatively short data set. We have now updated the relevant information on temperature in section 3.2.2 (pp8, lines 21-46) and included an extended discussion in Discussion and Summary (pp15, lines 1-23). However, we would prefer to abstain from further discussion, to avoid speculation. If the reviewer has a certain opinion on this issue, it might be helpful to receive a more elaborate suggestion.**

9. Results: the differences between CM2.5 and CMIP5 models in projecting the paper Mediterranean climate are explained with a) better representation of the SNAO teleconnection and b) improved representation of the land-atmosphere interaction by the LM3 model (see also the Abstract). However, the improvements of the LM3 model are not presented in the paper, nor how these new features actually improve the representation of the land-atmosphere interactions (*e.g. representation of soil moisture, evapotranspiration, albedo*). A brief presentation of the LM3 model as well as a discussion of how it improves climate simulation in the Mediterranean is needed.

**AU: Thank you for bringing up this gap in our writing. We have clarified the Abstract, added references to the data section (pp 3, lines: 41-46, pp4, lines: 1-9), and added text to the Discussion and Summary section (pp 16, lines 34-46) relating to land model improvements and some research highlighting LM3 performance. We agree that more analysis is required to further support this claim, which would add significant text and figures to the paper. We have included references of studies beginning to look into this problem, but have left the exploration of land-atmosphere interactions of the SNAO using LM3 for future research.**

Added references:

Berg, A., B.R. Lintner, K. Findell, S.I. Seneviratne, B. van den Hurk, A. Ducharne, F. Chéruy, S. Hagemann, D.M. Lawrence, S. Malyshev, A. Meier, and P. Gentine, 2015: Interannual Coupling between Summertime Surface Temperature and Precipitation over Land: Processes and Implications for Climate Change. *J. Climate*, 28, 1308–1328, <https://doi.org/10.1175/JCLI-D-14-00324.1>

Berg, A., Findell, K., Lintner, B., Giannini, A., Seneviratne, S. I., Van den Hurk, B., Ruth Lorenz, Andy Pitman, Stefan Hagemann, Arndt Meier, Frédérique Cheruy, Agnès Ducharne, Sergey Malyshev & P. C. D.

Milly, 2016: Land–atmosphere feedbacks amplify aridity increase over land under global warming. *Nature Climate Change*, 6(9), 869.

Milly, P.C., S.L. Malyshev, E. Shevliakova, K.A. Dunne, K.L. Findell, T. Gleeson, Z. Liang, P. Phillipps, R.J. Stouffer, and S. Swenson, 2014: An Enhanced Model of Land Water and Energy for Global Hydrologic and Earth-System Studies. *J. Hydrometeor.*, 15, 1739–1761, <https://doi.org/10.1175/JHM-D-13-0162.1>

10. Conclusions: most of the paper is devoted to the analysis of the SNAO teleconnection and its impact on future climate change in the Mediterranean, which show a significant (P17, Figure 11) impact on precipitation in southern Europe. And in the abstract you indicate this as one of the main results of the paper. Conversely, in the Conclusions you somehow reduce the importance of the SNAO impact (P22, L38-40), explaining the differences with the CMIP5 simulations as a consequence of the improved land model. This point needs to be clarified.

**AU: Following the reviewer’s suggestion, we have clarified the main message of the manuscript. We agree that the analysis of the impacts of the SNAO teleconnection consumes a significant part of the manuscript. This part shows a significant contribution of the SNAO to precipitation over southern Europe. However, the comparison of the SNAO impacts between CM2.5 model and CMIP3/CMIP5 models suggests that the SNAO cannot explain the difference in the future projections between these models. The apparent stark contrast between the CMIP3/CMIP5 and CM2.5 regional projections could more likely originate from the enhancements in the LM3 land model incorporated to CM2.5 at high spatial resolution, rather than the impacts of the SNAO. The relevant discussion is included in Discussion and Summary: pp16, lines:34-46, pp17 lines: 1-13. Future work should focus on understanding differences in land surface responses in this region to the SNAO and projected climate change.**

Minor comments:

P2, L15: the connection between the Mediterranean and the African monsoon has been robustly described as Mediterranean → Africa (see papers by Raicich et al. 2003 and Rowell 2003 [[https://doi.org/10.1175/1520-0442\(2003\)0162.0.CO;2](https://doi.org/10.1175/1520-0442(2003)0162.0.CO;2)]).

The influence of the African monsoon on the Mediterranean is less clear: Ziv et al. 2004, but also Fontaine et al. 2011 [<https://doi.org/10.1002/joc.2108>], actually find a link between convection in Africa and subsidence in the Mediterranean, however the mechanism is still not clear (see Gaetani et al. 2011 [<https://doi.org/10.1029/2011GL047150>]). Indeed, the Asian monsoon could be dominant in modulating the Mediterranean-Africa connection. Please modify the sentence to account for this aspect.

**Thank you for the comment. We found and included all the missing references, and modified the sentence (Raicich et al. 2003 and Rowell 2003, Fontaine et al. 2011) (pp 2, lines: 14-17).**

P2, L26-29: please add a reference.

P3, L18-20: please add a reference.

**Thank you, we add the references.**

P3, L43: “fixed levels of radiative forcing”, do you mean ‘radiative forcing from fixed levels of emission/concentration’?

**Thank you, the updated information is now included in pp: 4, lines 16-21.**

P4, Methods: is the model fully coupled? How many vertical levels are in the ocean model?

**We have updated the information (pp 4, lines: 1-9).**

P6, L15-16: this sentence should be moved to the Results section. **Thank you, we have applied the suggestion.**

P6, L18-19: what do you mean with “vector time series”? The time series of the vector containing spatial data? **Correct.**

P7, L39: from Figure 4, precipitation magnitude is actually, not “apparently”, larger than observations.

**We have corrected and rewritten the paragraph. (pp 7, lines 1-11)**

P7, L45: “none of the CMIP5. . .” **We have rewritten the relevant paragraph.**

P8, L1: do you mean that the CM2.5 runs in the CMIP5 archive are better than other models in the archive? Or do you refer to the runs you analyse in this paper? If this is the case, you should provide a figure to support this statement.

**Thank you. We referred to the CMIP5 analysis shown in Kelley et al. (2012). We have clarified this and add the reference where appropriate (pp3, lines: 9-14).**

P8, L10-13: when discussing the impact of NAO and SNAO on European climate, add references.

**Thank you. We have added the references throughout the paper.**

P8, L17: “and rather wet conditions”.

**Thank you, we applied the correction (pp 2, line 3).**

P8, L18-19: add references on future projections of SNAO.

**This paragraph is now rewritten. We have updated the references on future projections of SNAO (pp10, lines: 8-12, pp 14, lines 27-29, pp 15, lines 42-43).**

Section 3.2: the objective is to test the capability of the model in simulating the SNAO as an independent internally-generated mode of climate variability. However, the long introduction at P8-9 does not actually help in understanding why this is necessary. Is the internal variability modulated at multidecadal time scales? Is this modulation externally forced? Please try to clarify motivations and objectives of the section.

**Thank you, we have rewritten and clarified the section (pp7, line 16 - pp8, line 46). Part of the information has been moved to Introduction. As stated in the introduction of section 3.2, the purpose is to analyze the capability of the CM2.5 model to simulate the SNAO as an independent, internally generated climate component, which would prove the physical validity of the statistically-derived component. The “internally-generated” means that that the modulation is generated by the internal climate variations and it is not externally forced. However “the origin of the multi-decadal signal of SNAO has been linked (Knight et al. 2006, Folland et al 2009, Linderholm and Folland 2017) to the Atlantic Multidecadal Oscillation, which originates from internal variations in thermohaline circulation (Knight et al. 2005, 2006, Delworth and Mann 2000; Enfield et al. 2001), but for the recent decades also from anthropogenic sources (Rotstayn and Lohman 2002; Mann and Emanuel 2006).”**

P8, L20-26: this paragraph is confusing: on the one hand, it is true that different approaches/datasets may lead to uncertainty in the observed SNAO-Mediterranean teleconnection; on the other hand, uncertainties in model simulations originate from model shortcomings. Therefore uncertainty in the real and model worlds could originate from both intrinsic non-linear nature of the phenomenon and inadequate statistical/modelling tools. Please rephrase.

**Yes, we have substantially shortened and clarified this section. Additional discussion is included pp 15, lines 1-23.**

P9, L8-9: I cannot understand why and how anthropogenic forcing should intensify SNAO contribution (to the summer atmospheric circulation over North Atlantic). Please explain.

**We have substantially rewritten this section and this sentence is not included. The relevant information is included in pp15, lines 38-46, pp10, lines: 8-12.**

P9, L34: add the figures for July and August to the Supplement.

**We won't add this figure to the Supplementary Information, which already contains 10 supplementary figures, but we have updated the information that the figure is not attached.**

P9, L35: what is the interest of comparing with the HadCM3 model?

**This section analyzes the capability of CM2.5 in simulating SNAO and compares it with the available results of other models, in this case HadCM3 and HadGEM1 in Folland et al. 2009.**

P9, L42: is it HadGEM1 or HadCM3?

**The statement is correct.**

P13, L6-7: why an East Mediterranean index is used to compute correlation in Figure 8d, instead of the first EOF for NCEP omega? **The figure (in the current version Figure 6d) shows the correlations computed based on three-decade time series of NCEP omega at the mid-atmospheric level. Taking into account the relatively short length of the data set (compared to 1000 years CTRL run) and a relatively smaller plausibility of the data at the middle and higher atmospheric levels, we refrain from applying an EOF analysis to the NCEP dataset. In our consideration, applying an EOF analysis to such a short time series could lead to degeneracy of the derived eigenvalues. In other words, the EOF mode derived from the NCEP dataset could be easily a spurious combination of several modes, rather than a realistic representation of the SNAO mode.**

P14, L25-26: what do you mean with “estimated at the original model resolution”? Do you mean “computed”? **Thank you. The section is substantially rewritten and the sentence is removed.**

P14, L32: east. **We have applied the correction (pp 10, line 10)**

P17, L1-3: I don't understand why you refer to Fig. 10a (showing end-of-century projections) to discuss changes in SNAO. You could maybe use this figure to support your analysis of future SNAO.

**The figure shows the projected future changes (please note that in the current version this is Figure 7) and indeed we are using this figure to support the analysis of future SNAO (although it supports also the interpretation of the analysis of the already observed SNAO changes). The fingerprint of the future changes, derived from the sea level pressure projections, is consistent with the observed evolution of SNAO and thus it may constitute a possible contribution of the anthropogenic component already observed in the 20<sup>th</sup> century. We have tried to clarify this issue in the manuscript (pp 11, lines: 9-28).**

P17, L14-16: it would be preferable to present the regression method to estimate the SNAO impact here rather than in the Method section.

**Yes, the relevant information is now in the Methods section.**

P17, L43: “warming is lower over . . . than . . .”

**Thank you, we have substantially rewritten and improved this section.**

P18, L7-12: it is not clear to me whether you are discussing your results (in Figure 10) or previous findings. If you discuss your results, please add more references to Figure 10, otherwise add a reference to a paper.

**Yes, we have clarified the paragraph.**

P20, L39-41 and 42-45: please add references.

**Thank you, we have updated references in the section.**

P21, L20: “preindustrial value”.

**We have substantially shortened and clarified whole section, the relevant sentence is removed.**

P22, L9-10: please add a citation to CMIP5 results.

**Thank you, have updated the references where needed.**

Figures: for better comparison, figures presenting climate change in the Mediterranean should share the same geographical boundaries. Same recommendation for figures presenting SNAO and Asian monsoon teleconnections, respectively.

**Unfortunately this idea is not feasible and doesn't serve the purpose of the analysis. Each figure is presented in different context. For example, projected future changes for SLP are discussed in the context of the Euro-Atlantic climate. In contrast, regarding precipitation and temperature we want to focus on the Mediterranean region, but also discuss it from the perspective of climate in Europe. We have thoroughly reconsidered the way each figure is presented.**

Figure 6: what do contours represent? The sign looks reversed with respect to the standard SNAO pattern. Could you please fix this, not to mislead the reader?

**We have improved the figure and presented the SNAO at its positive phase. We have included the clarifying information in the caption. However, we would abstain from labeling the positive or the negative phase to a “standard pattern”.**

Figure 7: does it make sense to project the SNAO index derived from 20CR onto NCEP data? Why not just analyse one dataset?

**We agree with the reviewer that it is usually easier to use just one data set. However for the sake of consistency with an earlier part of the analysis, we used the 20CR dataset instead of the NCEP dataset. In the earlier part of the analysis we used the 20CR dataset, because the alternative ones, such as NCEP-NCAR1 or NCEP –DOE, would be too short for the analysis of the evolution of SNAO during the 20<sup>th</sup> century.**

Figure 8: Do you perform EOF on omega 500 and 300 together? Or is EOF analysis performed separately on omega 500 and 300? If this is the case, which time series do you use for correlations?

**Yes, the EOF analysis is performed separately for each level. The method is described in the manuscript but we will clarify and highlight this information also in the caption (Figure 6, pp5, lines 33-35).**

Figure 10: wind is displayed at which level? Is not model resolution 0.5?

**Thank you, we have included the missing information and applied the correction (Figure 7).**

Figure 11: in panels d and e you show regressions, while in Fig. 9c you show correlations.

**Figure d and e doesn't show regressions, but the projected changes. The impact of the SNAO in figure e is removed using linear regression. We have clarified the figure the caption.**

Figure 12: is omega at 200 or 500?

**It is omega at 500 hpa. The information is now updated (Figure 9).**

See P18, L23. Supplement: please follow the logical order of the paper to number the figures. Also please write complete captions, avoiding to refer to captions in the main text.

**Thank you for all the comments and advice regarding the figures.**



Dear editor,

I have read this paper and think it fits the scope of ESD. Moreover, I think the material presented in the paper is a welcome addition to the knowledge on climatic changes in the Mediterranean. My main issues with the current manuscript are in the presentation. I think it is quite long and should be more focused, possibly with a reduction in the number of figures.

Kind regards,

**AU: We thank the reviewer for their very thorough revision comments and feedback regarding our manuscript. We have addressed all of the major comments when revising the manuscript. This includes either applying the reviewer's suggestion or a thorough justification for not doing that. We have also made an effort to address the minor comments. Overall, we have reworked the text of the manuscript to improve its conciseness and clarity. The manuscript is shortened by ~20%. The main focus of the study, described in Introduction, is clarified. The key messages of the study, presented in Discussion and Summary, are clarified and enhanced. The number of figures is reduced from 12 to 10, by merging Figure 1 and 2 (in the previous version) into Figure 1, and Figure 8 and 9 (in the previous version) into Figure 6. We have also reworked the structure of the manuscript, so the text discussing the results is now included in Discussion and Summary. We have clarified the abstract.**

**We have also removed the discussion of the North Atlantic storm track, and the relevant figure (Figure 7 in the previous version of the manuscript). This part of the discussion will be very important in the further study that investigates the impact of the SNAO on northern Europe, but it is of minor importance for the Mediterranean hydroclimate investigated in the current manuscript.**

Specific comments:

1. The paper is quite long and elaborate, maybe wise to focus a bit more and reduce the number of figures?

**AU: Thank you for the comment. Following the reviewer's suggestion we have worked on the manuscript to make it more comprehensible. Particularly, we have reworked the introduction, the results and the discussion of the previous studies in a more concise way (section 3.2.1 and 3.2.2). The relevant information on the Mediterranean climate moved from sections 3.2 and 3.3 to the Introduction (pp2: lines 10-22). We have also removed the figure with storm tracks.**

2. There are many long sentences throughout the paper, which make it hard to follow the reasoning sometimes. I suggest to have a good look at opportunities to shorten them.

**AU: Thank you. We have improved the readability of the Introduction, Methods, Results and Summary.**

3. In many places in the manuscript, geographic names (Levant, Asia Minor, Balkans, Sahara, North Africa, EMED, and many more) are used to describe the model results. This assumes that the reader knows the location of all these places, which is probably not true. I suggest to indicate the relevant places in a figure and to be more specific in the geography when mentioning other places.

**AU: Thank you. We have described the necessary regions in the Methods section, and provided the specific locations (pp 5, lines: 1-6, 14-29).**

4. You compare the high resolution model output to NCEP/DOE reanalysis of 2.5

degree resolution. Why not compare it to higher resolution products, such as ERA5?

**AU:** Thank you for the comment. Incorporating datasets with higher resolution would not necessarily serve the purpose of the analysis of the large-scale circulation features. We have included below an additional figure (Figure R2), depicting sea level pressure and wind vector at 850hPa both in ERA-I and ERA 20CR, showing very good agreement between the suggested observational datasets.

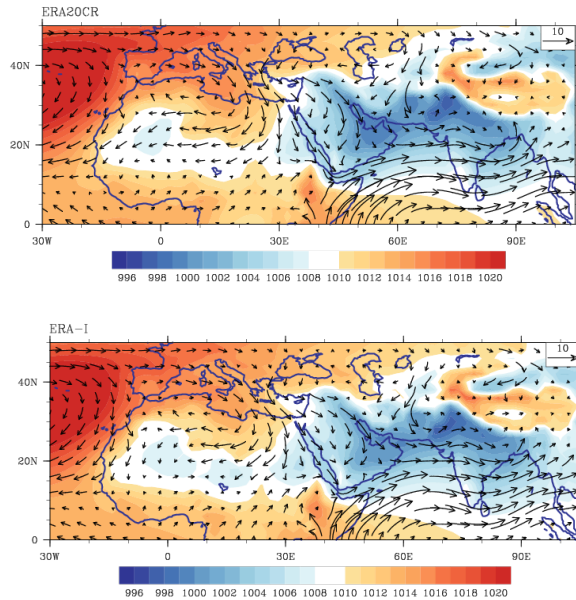


Figure R2. Seasonal (JJA) sea level pressure (hPa) and wind vector at 850hPa (m/s) in (top) ERA-20C, (bottom) ERA-I; for the 1979-2017 period.

**However a verification of the precipitation results with higher resolution datasets would improve the robustness of the conclusions. Following the reviewer's suggestion we have incorporated EOBS dataset in the analysis of the regional precipitation (Figure 3 in the current version). EOBS provides high quality data and serves as a good reference for the regional precipitation. Given the same spatial resolution as CM2.5, EOBS allows for comparing very fine features over the complex orography of the Mediterranean.**

5. Is there a significant difference between the top and bottom panels in Fig 7? It is not clear to me, maybe use a different color scale?

**AU:** Thank you. Yes, there is a significant difference between the top and bottom correlations (but not the storm track patterns), computed between the stormtrack proxy and the SNAO index. For example, negative correlations over northwest Europe in the 1970-2011 (bottom) are weaker than -0.5, while the correlations in 1950-1990 (top) are stronger than -0.65. The difference in the computed correlations questions the robustness of the SNAO (not the storm tracks), derived from the recent three-to four decades.

**Nevertheless, we have decided to remove this figure and the relevant discussion from the manuscript. The SNAO teleconnection with hydroclimate in northwestern Europe can be directly explained with variations in large-scale circulation over the North Atlantic and associated variations in storm tracks (as shown in observations and simulations in Folland et al. 2009). However, in this manuscript we do not intend to investigate the simulated impacts of SNAO on the North-Atlantic storm tracks and the northwestern Europe hydroclimate. This topic will be investigated in a further study. We have clarified the text (pp8, lines: 37-41) and also the main focus of the study (in Introduction, pp3, lines:**

20-37). To maintain brevity, we have removed the figure representing the variations in storm track.

6. Indicate different data sources (HIST, PROJ runs) in Fig 11c? Maybe by a vertical line in the plot?

**AU: Thank you, we have included the vertical line in the figure (Figure 8 in the current version).**

7. P21L35, "This may stem from...". I agree that the anthropogenic forcing is not included in the control run and may contribute to this discrepancy. But what about other explanations?

**AU: Please note that we have substantially rewritten and clarified the Summary and Discussion section (pp15, lines 1-23). We also included more information in Introduction (pp2, lines 1-12):**

**“The origin of the multi-decadal signal of SNAO has been linked (Knight et al. 2006, Folland et al 2009, Linderholm and Folland 2017) to the Atlantic Multidecadal Oscillation, which originates from internal variations in thermohaline circulation (Knight et al. 2005, 2006, Delworth and Mann 2000; Enfield et al. 2001), but for the recent decades also from anthropogenic sources (Rotstayn and Lohman 2002; Mann and Emanuel 2006).”**

**We would like to provide a more thorough explanation for the apparent better agreement between the observed and simulated SNAO before 1980s than for the later period:**

**This may stem from the fact that the SNAO component derived for the simulated and observed recent decades (1980s-2010s) could be to a large extent conditioned by a coincidence of the multidecadal scale internal (unforced) variability and multidecadal anthropogenic forcing. Taking into account the random nature of the unforced climate variations, their temporal evolution in the simulated 1980's-2010's period may look very different from the observed one. In the presence of an additional long-term component, such as anthropogenic forcing, the EOF analysis (which is set to extract a signal explaining a maximum variance) is likely to choose a combination of a random representation of the unforced variability and the anthropogenic forcing. This combination (regarded as the SNAO component) may have a very different form in the observations and simulations.**

1 **Changes in the future summer Mediterranean climate: contribution of teleconnections**  
2 **and local factors.**

3  
4 Monika J. Barcikowska<sup>1</sup>, Sarah B. Kapnick<sup>2</sup>, Lakshmi Krishnamurty<sup>3</sup>, Simone Russo<sup>4</sup>,  
5 Annalisa Cherchi<sup>5</sup>, Chris K. Folland<sup>6,7,8</sup>

6  
7 <sup>1</sup>Environmental Defense Fund, New York City

8 <sup>2</sup>Geophysical Fluid Dynamics Laboratory, National Oceanic and Atmospheric Administration, 201 Forrestal  
9 Road, Princeton, NJ 08540, USA

10 <sup>3</sup>Princeton University, GFDL Princeton University Forrestal Campus, 201, Forrestal Road, Princeton, NJ  
11 08542, USA

12 <sup>4</sup>European Commission, Joint Research Centre, Via Enrico Fermi, Ispra, Italy

13 <sup>5</sup>Fondazione Centro Euro-Mediterraneo sui Cambiamenti Climatici, and Istituto Nazionale di Geofisica e  
14 Vulcanologia, Bologna, Italy

15 <sup>6</sup>School of Environmental Sciences, University of East Anglia, Norwich, UK

16 <sup>7</sup>Department of Earth Sciences, University of Gothenburg, Sweden

17 <sup>8</sup>International Centre for Applied Climate Sciences, University of Southern Queensland, Australia

18  
19  
20 **Abstract**

21 This study analyzes future climate for the Mediterranean region, projected with the high-resolution coupled  
22 CM2.5 model, which incorporates a new and improved land model (LM3). The simulated climate changes  
23 suggest pronounced warming and drying over most of the region. However, the changes are distinctly smaller  
24 than those of the CMIP5 multi-model ensemble. In addition, changes over much of southeast and central  
25 Europe indicate very modest warming compared to the CMIP5 projections and also a tendency to wetter  
26 conditions. The differences between CM2.5 projections of future changes and those of previous-generation  
27 models indicates a possible role of other factors such as land surface-atmospheric interactions, in particular  
28 over central and southeastern Europe. Our analysis also highlights the importance of correctly projecting the  
29 magnitude of changes in the summer North Atlantic Oscillation, which has the capacity to partly offset  
30 anthropogenic warming and drying over the western and central Mediterranean. Nevertheless, the projections  
31 suggest a decreasing influence of local atmospheric dynamics and teleconnections in maintaining the regional  
32 temperature and precipitation balance, in particular over arid regions like the eastern and southern  
33 Mediterranean, which show a local maximum of warming and drying. The intensification of the heat low in  
34 these regions suggests rather an increasing influence of warming land surface on the local surface atmospheric  
35 circulation and progressing desertification.

36  
37  
38 **1. Introduction**

39  
40 The climate in the Mediterranean region is primarily characterized by mild, wet winters and hot, dry summers.  
41 However, the complex geomorphological characteristics including gulfs, peninsulas, islands, the mountain  
42 ridges surrounding the Mediterranean Sea basin, as well as the influence of the mid-latitude and tropical  
43 atmospheric circulation patterns translate into a distinctively complex climate.

44  
45 The influence of the mid-latitude circulation on the regional hydroclimate is mostly manifest in the  
46 teleconnection with the North Atlantic Oscillation (e.g. Hurrell, 1995, Krichak et al. 2002, Barcikowska et al.

1 | 2017b). The summer expression of the NAO (SNAO, Folland et al. 2009, Linderholm et al., 2009, Blade et al.  
2 | 2012), in its positive SNAO phase yields a stronger meridional SLP gradient over the North Atlantic, an  
3 | enhanced anticyclonic southern lobe with dry conditions over northwest Europe and rather wet conditions  
4 | over the central Mediterranean. The SNAO has been linked to the Atlantic Meridional Oscillation (Knight et  
5 | al. 2006, Folland et al 2009, Linderholm and Folland 2017), which originates from both internal ocean  
6 | variations (Knight et al. 2005, 2006, Delworth and Mann 2000; Enfield et al. 2001), and anthropogenic  
7 | sources (Rotstayn and Lohman 2002; Mann and Emanuel 2006). However, current literature has not yet  
8 | reached a full consensus on the spatial definition (fingerprint), origin and impacts of the SNAO. The results of  
9 | observational analysis vary, depending on the chosen data set, period, summer season interval, and the  
10 | analysis method (Barnston and Livezey, Hurrell and van Loon 1997, Hurrell and Folland 2002; Hurrell et al.  
11 | 2003, 2009, Cassou et al. 2005, Folland 2009, Blade 2012). This sensitivity stems largely from the  
12 | pronounced interannual-to-multidecadal variability of the observed SNAO.

Monika Barcikowska 7/19/19 3:32 PM

**Deleted:** are the main manifestation of mid-latitudes influence for winter precipitation in the northern parts of the region.

14 | In the summer, the northward shift of the Hadley cell reveals a connection between the hot and arid eastern  
15 | part of the Mediterranean and the Asian and African monsoons, as well as a possible connection between  
16 | these two monsoons (Rodwell and Hoskins 1996, Ziv et al. 2004, Fontaine et al. 2011, Raicich et al. 2003,  
17 | Rowell 2003).  
18 | Thermal balance of the central-eastern part of the Mediterranean is largely maintained by the two dynamical  
19 | factors, i.e. the cool air advection of the low-level northerly winds (i.e. Etesians, HMSO 1962; Metaxas 1977;  
20 | Maheras 1980; Prezerakos 1984; Reddaway and Bigg 1996; Zecchetto and de Biasio 2007; Chronis et al.  
21 | 2011) and the adiabatic warming of the mid- and upper level subsidence winds (Raicich et al. 2003, Mariotti  
22 | et al. 2002, Tyrlis et al. 2013), which counterbalance each other. Ziv et al. 2004 have shown these two factors  
23 | to be significantly correlated, pointing to the Asian Summer Monsoon which exerts an influence on the  
24 | Mediterranean surface-, mid- and upper-troposphere dynamics. The possible mechanism behind this linkage  
25 | was explored in a framework of the Rossby wave pattern response to the diabatic heating of the monsoon  
26 | convection, i.e. monsoon-desert mechanism (Rodwell and Hoskins, 1996, Tyrlis et al. 2013, Rizou et al. 2015,  
27 | Cherchi et al. 2014, Cherchi et al. 2016). Additionally, Rodwell and Hoskins 2001 explained changes of  
28 | Etesian winds as a direct result of changes in the subsidence over EMED, which via Sverdrup's equation  
29 | controls the low-level northerly flow.

Monika Barcikowska 7/17/19 6:41 PM

**Deleted:** The regional summer climate features a seasonal minimum of the rainfall, persistent mid-level and upper-level subsidence and low-level northerlies (Raicich et al. 2003, Mariotti et al. 2002) centered over the central-eastern part of the Mediterranean. The low-level northerlies are called

Monika Barcikowska 7/19/19 3:03 PM

**Deleted:** Etesian winds (HMSO 1962; Metaxas 1977; Maheras 1980; Prezerakos 1984; Reddaway and Bigg 1996; Zecchetto and de Biasio 2007; Chronis et al. 2011) and they result from the zonal pressure gradient forged by the Atlantic subtropical anticyclone and the western flanks of the Asian monsoon heat low (Bitan and Saaroni 1992; Saaroni and Ziv 2000; Alpert et al. 2004; Saaroni et al. 2010).

31 | The geographic location and socio-economic state of the Mediterranean make, the population in this region  
32 | particularly vulnerable to climate change. The southern part of the Mediterranean, which is dominated by  
33 | agricultural activities, is especially sensitive to prolonged water shortages and their consequences, such as  
34 | drought and wildfires. Giorgi (2006) found this region to be particularly responsive to projected climate  
35 | change and identified it as a climate hot spot. In fact, both CMIP3 (Giorgi and Lionello 2008, Hanf et al.  
36 | 2012) and CMIP5 future projections for this region (Diffenbaugh and Giorgi 2012, Alessandri et al. 2014,  
37 | Mariotti et al. 2015, Feng et al. 2014) indicate very strong warming and reductions in precipitation during the  
38 | summer season. These changes can severely impact water and food security.

Monika Barcikowska 7/17/19 7:20 PM

**Deleted:** The cool air advection of the Etesian winds counterbalances the adiabatic warming of the mid- and upper level subsidence, maintaining in this way a thermal balance over the eastern Mediterranean

Monika Barcikowska 8/19/19 4:32 PM

**Deleted:** s

Monika Barcikowska 8/23/19 5:16 AM

**Deleted:**

Monika Barcikowska 8/19/19 4:33 PM

**Deleted:** a

41 | At the same time, observational studies have yet to find unambiguous evidence of decreasing precipitation in  
42 | recent decades (Blade et al. 2012b, Giorgi and Lionello 2008). Moreover, some studies (e.g. Christensen and  
43 | Boberg, 2012, Mueller and Seneviratne, 2014) indicated that the projected in CMIP3 and CMIP5 future  
44 | warming is spuriously amplified by a strong summertime positive bias, caused by the deficiencies in the  
45 | simulated atmosphere - land surface feedbacks. Moreover, Seneviratne et al. (2006) identified soil moisture-  
46 | temperature feedbacks as a dominant factor controlling summer temperature variability in the Mediterranean  
and Central Europe in a changing climate. Soil moisture-climate feedbacks were also linked to non-linear

Monika Barcikowska 7/24/19 3:31 PM

**Formatted:** Widow/Orphan control, Adjust space between Latin and Asian text, Adjust space between Asian text and numbers

Monika Barcikowska 8/19/19 4:33 PM

**Deleted:** a



1 warming of hot extremes in climate change projections for the Mediterranean (Diffenbaugh et al. 2007).  
2 Hirschi et al. (2011) confirmed the effect of soil moisture availability for hot extremes in observations in  
3 Southeastern Europe and found also that the soil moisture-temperature feedbacks in RCMs are often  
4 overestimated over Central Europe.

5  
6 [Cherchi et al. \(2016\)](#) also confirmed also that the projected in CMIP5 future severe warming over the eastern  
7 Mediterranean can not be explained with the impact of South Asian monsoon teleconnection, maintained via  
8 monsoon – desert mechanism. On the other hand, [Blade et al. \(2012\)](#) argued that the regional warming and  
9 drying projected in CMIP3, is caused by the misrepresentation of the summer NAO teleconnection. Kelley et  
10 al. (2012) indicated that CMIP5 models show a rather modest improvement in the simulated regional  
11 hydroclimate, compared to CMIP3. The CMIP5 historical simulations still differ from the observations, for  
12 example by showing a strong wetting over the northwestern parts of Europe and drying over the southwestern  
13 parts of the Mediterranean (e.g. Kelley et al. 2012), though some earlier lower resolution models do show  
14 strong drying over many, though not all, parts of north west Europe as well (e.g. Rowell and Jones, 2006).  
15 The inconsistencies [found between the observations and simulations](#) do not add to the credibility of the  
16 current future projections for the Mediterranean and [prompt](#) further investigation, [using](#) higher resolution  
17 models [and also advanced understanding of the land surface–atmosphere feedbacks as well as the regional](#)  
18 [teleconnections](#).

19  
20 [In this study we analyze the future summer climate over the Mediterranean, projected with the GFDL CM2.5](#)  
21 [model \(Delworth et al., 2012\) that incorporates higher spatial resolution \(~50km\) and improved land model](#)  
22 [\(LM3\), likely improving the simulated hydroclimate over many continental regions including Europe. The](#)  
23 [analysis aims to interpret the derived future climate changes through the prism of contributing SNAO](#)  
24 [teleconnection, as well as the impact of local surface warming and the associated land surface-air interactions.](#)

25  
26 Section 2 describes the [model and experiments used, the dataset for comparison](#) and the methodology. Section  
27 3 focuses on the summer time-mean climatology of the region, as well as its teleconnections. It evaluates the  
28 performance of the model in terms of the simulated regional precipitation, as well as large-scale circulation  
29 features, which shape the summer regime of the Mediterranean climate. It also examines the [capacity of the](#)  
30 [model to simulate the SNAO and its impact on the Mediterranean climate](#). The last part of this section focuses  
31 on a representation of [the key dynamical features of the eastern Mediterranean climate](#), i.e. the linkage  
32 between the mid- and upper-level subsidence and the low-level [northerly flow](#) (and the associated Etesian  
33 winds) together with its coupling with the Indian Monsoon. Section 4 investigates future climate changes over  
34 the Mediterranean derived from [the model](#) projections. It examines the regional changes from the perspective  
35 of [a\) large-scale circulation over the Euro-Atlantic and the influence of the SNAO teleconnection, b\) local](#)  
36 [land surface warming and its influence on the climate regime of the eastern Mediterranean](#). Section 5  
37 discusses and summarizes the main results.

## 38 [2. Data and Methods](#)

### 39 [2.1 Coupled model and experiments](#)

40 The coupled model used in this study is the Geophysical Fluid Dynamics Laboratory (GFDL) CM2.5. It has  
41 an atmospheric and land surface horizontal grid scale of approximately 50 km with 32 levels in the vertical.  
42 The horizontal grid scale of the ocean increases from 28 km in the tropics to 8-11 km in high latitudes. CM2.5  
43 [incorporates](#) a new land model (LM3), with enhanced representation of soil moisture and land-atmospheric  
44 feedbacks between soil moisture and precipitation (Milly et al. 2014, Berg et al. 2016). Details of the CM2.5  
45 model features can be found in Delworth et al. (2012). [The representation of the summer precipitation](#)  
46

Monika Barcikowska 7/19/19 6:31 PM

**Deleted:** main components of internal variability dominating atmospheric circulation over the Euro-Atlantic region, such as the summer NAO,

Monika Barcikowska 7/19/19 6:35 PM

**Deleted:** The derived regional changes are also interpreted in the context of the changing relationships between the dynamical factors governing

Monika Barcikowska 7/19/19 6:55 PM

**Deleted:**

Monika Barcikowska 7/19/19 7:04 PM

**Deleted:** Again, the long control run is used to verify whether the derived changes in the eastern Mediterranean climate regime can be attributed to the local effects of the warming Mediterranean and how these effects will impact the whole Mediterranean and European climate.

Monika Barcikowska 7/19/19 6:44 PM

**Formatted:** Font:(Default) Times New Roman

Monika Barcikowska 7/19/19 6:24 PM

**Deleted:** [...](#) [1]

Monika Barcikowska 8/19/19 9:44 AM

**Formatted:** Font:Bold

Monika Barcikowska 8/19/19 4:27 PM

**Deleted:** an

1 | [climatology in CM2.5](#) is also compared using a 4000-years control run of GFDL CM2.1, that is the CM2.5's  
2 | predecessor. CM2.1 incorporates a grid scale of 2° latitude x 2.5° longitude for the atmosphere. The ocean  
3 | resolution is variable being approximately 1° latitude x 1° longitude, with a finer meridional resolution in the  
4 | tropics. The CM2.1 atmospheric model has 24 vertical levels (Delworth et al. 2006). The ocean component  
5 | CM2.1 and CM2.5 consist of 50 levels in the vertical. Future changes projected with CM2.5 are compared  
6 | with that derived with the CSIRO-Mk3-6-0 model (1.9° x 1.9° horizontal resolution for the atmosphere),  
7 | which includes the ocean component based on the GFDL ocean model. This choice was determined by the  
8 | fact that future projections of CSIRO-Mk3-6-0 model, unlike CM2.1, follow the same protocol of forcing  
9 | scenario, i.e. the IPCC RCP8.5 scenario (Meinshausen et al. 2011, Riahi et al. 2011), as those of CM2.5.

Monika Barcikowska 7/19/19 6:24 PM  
Formatted: Font color: Auto

10 |  
11 | The set of experiments performed using CM2.5 are listed in Table 1 and it consists of control simulations  
12 | (hereafter CTRL) and 5-members ensembles of historical simulations (hereafter HIST), and of future  
13 | projections (hereafter PROJ) performed with CM2.5. The CTRL simulation consists of a 1000-year  
14 | integration, where greenhouse gas and aerosol compositions are held fixed at the levels of the year 1860. [In](#)  
15 | [HIST and PROJ ensembles](#), the forcing follows the protocols of the Coupled Model Intercomparison Project  
16 | Phase 5 (<http://cmip-pcmdi.llnl.gov/cmip5/forcing.html>). For [the historical period](#) (1861-2005), the radiative  
17 | forcings are based on observational estimates of concentrations of well-mixed greenhouse gases (GHG),  
18 | ozone, volcanoes, aerosols, solar irradiance changes and land-use distribution. [While for the future \(2006-](#)  
19 | [2100\) the radiative forcing follows](#) an estimate of projected changes defined in the IPCC RCP8.5 scenario.  
20 | This scenario assumes high population growth, slow technological change and energy intensity improvements,  
21 | and a lack of developed climate change policies, resulting in large energy demand and GHG emissions.

Monika Barcikowska 8/19/19 9:44 AM  
Formatted: Font:Bold

## 2.2 Datasets used for comparison

22 |  
23 | The simulated features of large-scale circulation are compared with reanalysis data of monthly pressure at  
24 | mean sea-level (hereafter SLP), wind vectors at the 850hPa and 200hPa levels, and vertical velocity at 200hPa  
25 | for the period 1979-2017. Reanalysis data is provided by the NCEP-DOE AMIP-II Reanalysis 2 with 2.5° x  
26 | 2.5° horizontal resolution and 17 vertical levels (Kanamitsu et al., 2002;  
27 | <https://www.esrl.noaa.gov/psd/data/gridded/data.ncep.reanalysis2.html>).

Monika Barcikowska 8/19/19 9:44 AM

**Deleted:** The relationship between the SNAO and the North Atlantic storm tracks derived by computing correlations between the SNAO index and the proxy of storm track in July-August. The storm tracks are represented with the standard deviation of the daily geopotential height at 300 hPa, following Folland et al. 2009. The data is a priori filtered using a Butterworth filter with a bandwidth of 2-8 days. The storm tracks are derived for the 1950-1990 and 1970-2011 periods, using NCEP/NCAR 1 data (Kalnay et al. 1996), provided by the NOAA/OAR/ESRL PSD, Boulder, Colorado, USA, from their Web site at <https://www.esrl.noaa.gov/psd/>.

Monika Barcikowska 8/19/19 9:44 AM

Formatted: Font:Bold

Monika Barcikowska 7/19/19 6:26 PM

Deleted: - ... [2]

28 |  
29 | The simulated precipitation is compared with the seasonal time-averaged precipitation provided by the  
30 | University of Delaware (V4.01), Legates and Willmott 1990; [http://climate.geog.udel.edu/~climate/html\\_pages/README.ghcn\\_ts2.html](http://climate.geog.udel.edu/~climate/html_pages/README.ghcn_ts2.html) (last access: July 2018). This is a global gridded land data set  
31 | with 0.5° x 0.5° horizontal resolution [for the period 1980-2015](#). [For the same period we use also EOBS](#)  
32 | [precipitation data set provided E-OBS dataset from the EU-FP6 project UERRA](#) (<http://www.uerra.eu>) and  
33 | the Copernicus Climate Change Service (Cornes et al. 2018, [version 17](#)), [provided at 0.25° x 0.25° horizontal](#)  
34 | [resolution](#).

35 |  
36 | The observational analysis of the summer North Atlantic Oscillation (section 3.2) is carried out using July-  
37 | August mean sea level pressure (SLP), provided by NOAA/ESRL PSD 20th Century Reanalysis version 2c  
38 | (Compo et al. 2006, [https://www.esrl.noaa.gov/psd/data/20thC\\_Rean/](https://www.esrl.noaa.gov/psd/data/20thC_Rean/)). The spatial patterns of the dominant  
39 | component of the SLP variations are computed with Empirical Orthogonal Function (EOF) analysis, over the  
40 | domain [25°-70°N, 70°W-50E°], following Folland et al. 2009. The robustness of the pattern is tested against  
41 | [chosen periods of different length](#).

## 2.3 Analysis methods

1 The representation of the simulated large-scale atmospheric circulation over the Mediterranean is analyzed  
2 using CTRL runs' monthly mean fields of the lower, mid- and upper- level dynamics over the region covering  
3 southern Europe, North Africa and South Asia [30°N–50°N, 30°W–110°E]. The analysis of the simulated  
4 SNAO teleconnection focuses on the Euro-Atlantic region. In the analysis of the eastern Mediterranean  
5 climate, we define [the region of focus as EMED \[30°-36°N, 36°-42°E\]. We will also refer to the eastern](#)  
6 [Mediterranean land region, which includes: Syria, Lebanon, Israel, Jordan, as the Levant region.](#)

7  
8 [The time-mean large-scale circulation features are analyzed based on the monthly means of hydro-](#)  
9 [meteorological variables for the summer \(June, July and August, hereafter JJA\) season.](#) Future changes are  
10 estimated by comparing the climatology at the end of the twenty-first century (i.e. 2061–2099, hereinafter  
11 future) of the RCP8.5 scenario with that at the end of the twentieth century (i.e. 1961– 1999, hereinafter  
12 present) of the historical simulation using monthly mean fields for [the summer](#) season.

13  
14 The teleconnection of the Mediterranean climate with SNAO is analyzed using the full (1000 year) CTRL run  
15 (section 3.2), as well as the historical and future runs. The SNAO is defined as a lead component of SLP  
16 vector time series over the Euro-Atlantic region [25°N–75°N, 70°W–50°E] in “core summer” (July-August),  
17 following Folland et al. 2009. [The choice of the time window is determined by the fact that the temporal](#)  
18 [behavior of the SNAO is significantly correlated only within these two months.](#) The impact of this  
19 teleconnection on Mediterranean climate is estimated using correlations between SNAO PC time series and  
20 the regional temperature and precipitation, [using the long CTRL experiments and the historical and future](#)  
21 [ensembles.](#) The evolution of the SNAO fingerprint in the 20<sup>th</sup> and 21<sup>st</sup> century is analyzed by projecting the  
22 vector time series of HIST and PROJ [experiments](#) (240 yrs, 1861-2100) on the SNAO eigenvector derived  
23 from the CTRL run. [To analyze potential changes in the spatial pattern of SNAO and associated impacts, the](#)  
24 [EOF analysis is applied independently to each of the HIST and PROJ ensembles, in the period 1950-2010 and](#)  
25 [2040-2100, respectively, detrending the time series before computing the EOF. In both epochs, the analysis](#)  
26 [has been](#) also tested for shorter periods (i.e. 50 and 30 years), which did not change the results in qualitative  
27 terms. Each of the five SNAO time series for the 1950-2010 and 2040-2100 periods [was](#) correlated with the  
28 respective detrended precipitation fields. [The results are compared with the observational analysis, using SLP](#)  
29 [provided by the 20CR dataset in the period 1870-2010.](#)

30  
31 The summer climate regime of the eastern Mediterranean (hereafter EMED) is examined from the perspective  
32 of the regional mid- and upper-tropospheric subsidence and its physical linkage with the surface circulation  
33 (section 3.3). The seasonal variability of the subsidence over the eastern Mediterranean is derived from  
34 EOF analysis applied to vertical velocity ( $\omega$ ) fields at 500 hPa, and also at 300 hPa [\(each level](#)  
35 [separately\)](#) over the region covering the Mediterranean, North Africa and [the Middle East](#) in July season. The  
36 physical linkage between the subsidence and surface circulation is estimated using correlations between the  
37 time series of the first EOF component (PC1) and the regional sea level pressure, geopotential height and  
38 wind vectors at 850 hPa. The relationship between the EMED region dynamics and the Indian Summer  
39 Monsoon is estimated by computing additional correlations with precipitation, outgoing longwave radiation,  
40 and the vertically integrated water column. [The analysis shows the correlations computed using time series of](#)  
41 [EOF omega at 500 hPa, but the correlations using EOF omega 300 hPa were almost the same. The results of](#)  
42 [the analysis are shown for July when the magnitude of subsidence and the Etesians is at its maximum and the](#)  
43 [response of the Rossby waves to monsoon rainfall is also strongest \(Tyrlis et al. 2012, Lin et al. 2007, Lin et](#)  
44 [al. 2009\). The results derived for June and August are shown in the Supplementary Information.](#)

45

Monika Barcikowska 8/19/19 4:23 PM

Deleted: ere

Monika Barcikowska 8/19/19 4:21 PM

Deleted:

1 Future changes in the dynamical linkages governing the summer climate regime over the eastern  
2 Mediterranean were analyzed by comparing the five-decade-long samples for July, i.e. 1960-2010 and 2050-  
3 2100. The linkage was calculated in a similar manner to that of the control run using correlations between the  
4 time series of the EOF over the EMED region subsidence and the atmospheric surface circulation fields. All  
5 EOF time series were computed by projecting the respective run on the eigenvector derived from the control  
6 run. The correlations were derived for each run (historical and future, respectively), using a priori detrended  
7 time series. The final result shows the ensemble mean for the five-member historical and future correlations.

Monika Barcikowska 8/19/19 4:19 PM  
Deleted:

8  
9 An additional analysis investigates the potential influence of the local temperature (i.e. in the EMED region)  
10 on the derived local dynamical relationships (section 4.3 and Supplementary Material). Therefore, the derived  
11 correlations were differentiated between samples with the 300 warmest and the 300 coldest summers (July)  
12 over the Mediterranean, chosen from the control run time series. Their selection is based on surface  
13 temperature in the EMED region. Additionally, a diagnosis of temperature impacts on the regional  
14 atmospheric circulation was performed using composite differences between the two temperature samples and  
15 the associated relative humidity, sea level pressure, wind components, geopotential height, vertical velocity  
16 and precipitation. The results were corroborated by testing their sensitivity to the precise choice of the region.

Monika Barcikowska 8/19/19 9:44 AM  
Deleted: -

### 18 3 Summer mean present climate and teleconnections over the Mediterranean region

#### 19 3.1 Simulated summer mean Mediterranean climate

20  
21 Figure 1a,b demonstrates that the model captures the subtropical low-tropospheric circulation with high  
22 fidelity when compared with the reanalysis (NCEP-DOE). It reproduces accurately the zonal pressure gradient  
23 over the Mediterranean, both in terms of pattern and magnitude, forged by the difference between the  
24 subtropical anticyclone over the North Atlantic and the massive Asian monsoon heat low. The latter extends  
25 westward, through the Arabian Peninsula towards the Levant region and southern Asia Minor. Concomitant to  
26 the zonal pressure gradient and adjustments to the regional orography is a persistent west-northerly flow over  
27 the central and eastern Mediterranean (i.e. the Etesian winds). The model reliably captures its local-scale  
28 features, created by adjustments to the regional topography. This includes a local wind maximum centered  
29 over the Aegean Sea and its southern extension reaching the Sahel region. These northerlies are also  
30 channelled through the Red Sea Straits and the Persian Gulf, reaching the Indian Ocean.

Monika Barcikowska 8/19/19 4:17 PM  
Deleted: n

Monika Barcikowska 8/23/19 5:59 AM  
Deleted: 2

Monika Barcikowska 8/19/19 4:17 PM  
Deleted: the

31  
32 Figure 1c,d shows that the model reproduces the location and magnitude of the summer subtropical mid-  
33 troposphere anticyclone, which spreads from the eastern Mediterranean across South Asia. The simulated  
34 mid-troposphere also captures the location and a realistic magnitude of the persistent mid-troposphere (500  
35 hPa) subsidence (positive omega) which creates the exceptionally hot and arid climate of the eastern  
36 Mediterranean. This subsidence gradually decreases towards the Iranian Plateau, which together with  
37 ascending motion over the South Asian monsoon region, creates a large-scale time-mean zonal gradient. The  
38 simulated zonal gradient is well shown (Figure 2a) by a vertical cross-section of vertical velocity (omega)  
39 averaged over 20°-34°N between the east Mediterranean region (positive omega means strong subsidence)  
40 and the South Asia (negative omega means ascending air). This characteristic gradient agrees well with its  
41 observational counterpart (Figure 2b) both in terms of magnitude and pattern. Importantly, the model captures  
42 the observed local maximum of the eastern Mediterranean subsidence located at middle-tropospheric levels  
43 (300-700 hPa), the region most sensitive to the impact of the Indian monsoon teleconnection.

Monika Barcikowska 8/23/19 5:59 AM  
Deleted: 3

Monika Barcikowska 8/23/19 5:59 AM  
Deleted: 3

44  
45 Figure 3 shows climatologies of the Mediterranean precipitation provided by the observations, the CM2.5  
46 control run, and also its low-resolution (CMIP3) predecessor, i.e. CM2.1 at their original horizontal

Monika Barcikowska 8/23/19 6:04 AM  
Deleted: 4

1 resolutions. Although both CM2.1 and CM2.5 depict the general spatial features of the climatology (i.e. large  
2 values in the northern Mediterranean, particularly over the Alps and the Balkans), the former introduces large  
3 biases (up to 50%) in [the](#) regions with sharp spatial gradients. CM2.5 [reproduces](#) precipitation [with a greater](#)  
4 [level of detail](#), clearly indicating the advantages of higher horizontal model resolution for regions with  
5 complex orography. However, precipitation magnitude in most mountainous areas, e.g. the northern Iberian  
6 Peninsula, the Alps and over Asia Minor, is larger than in [both](#) observational data sets, i.e. U. Delaware and  
7 [EOBS](#). [The climatology in CM2.5, in terms of pattern and magnitude, seem to be more consistent with the](#)  
8 [EOBS data set](#). [However](#), due to a [relatively large](#) observational uncertainty in many mountainous areas, it is  
9 difficult to validate the model rainfall climatology in these regions. Overall, our analysis indicates that the  
10 high-resolution CM2.5 control run [faithfully reproduces](#) the [mean](#) surface- and upper-tropospheric circulation  
11 over the Mediterranean [and it captures the complexity of the regional precipitation](#).

Monika Barcikowska 7/24/19 4:24 PM

**Deleted:** solves much better the spatial features of

### 14 3.2 The impact of the summer North Atlantic teleconnections [on the Mediterranean region](#)

16 [The imperative of the following section is to test the capability of the model to simulate the SNAO as an](#)  
17 [independent, internally generated climate component, which would prove the physical validity of the](#)  
18 [statistically - derived component](#). The analysis is applied to the full period (1000 years) of the CTRL  
19 [experiment \(Table 1\), repeated for the HIST and PROJ runs. The results are compared with the observational](#)  
20 [analysis, using SLP provided by the 20CR dataset in the period 1870-2010. However, allowing for the fact](#)  
21 [that a\) circulation over the SNAO region is influenced by different key factors at different times, giving rise to](#)  
22 [time-varying dominant modes of apparent internal variability; and b\) each simulation represents a different,](#)  
23 [non-deterministic state of internal climate variations, one should not expect to obtain from each run a replica](#)  
24 [of the observed SNAO component](#).

#### 26 3.2.1 Spatial pattern of SNAO

28 [The EOF analysis applied to the CTRL run results in two components, from which the first one clearly](#)  
29 [dominates the summer SLP variations, explaining twice as much total variance as the second one \(34% and](#)  
30 [15%, respectively\)](#). In the following, we focus on the leading pattern (hereafter called CTRL EOF1), [which](#)  
31 [represents the SNAO](#).

Monika Barcikowska 7/24/19 8:48 PM

**Deleted:** .

Monika Barcikowska 8/23/19 6:05 AM

**Deleted:** 5

33 Figure 4a depicts [the](#) spatial pattern of CTRL EOF1. The derived dipole resembles the observed SNAO  
34 signature (e.g. Folland et al. 2009), including a distinct northward shift when compared to the winter  
35 counterpart (shown e.g. in Barcikowska et al. 2017). The dipole pattern has a northern lobe over the south-  
36 western flank of Greenland and a southern lobe centered north of the Azores in the vicinity of ~45°N, 30°E.  
37 At its positive phase SNAO is manifest with negative anomalies in the former and positive anomalies in the  
38 latter region, thereby strengthening the meridional SLP gradient over the North Atlantic. The pattern is similar  
39 also when analyzed for the single months [of](#) July and August [\(not shown\)](#).

Monika Barcikowska 7/24/19 9:55 PM

**Deleted:** The simulated SNAO pattern is almost identical to the one derived from the HadCM3 model control run, as shown in Folland et al. 2009.

Monika Barcikowska 7/24/19 10:06 PM

**Deleted:** depicts patterns of EOF1's derived from four 50-yr periods of the 20CR reanalysis

41 Further analysis indicates also that the signature of the [simulated SNAO](#) is much more consistent with the  
42 observed one before [the](#) 1970s, rather than in the recent six decades. [The analysis of the leading EOF's](#)  
43 [derived from the consecutive periods of 20CR reanalysis \(50-yr periods i.e. a. 1870-1920, b. 1900-1950, c.](#)  
44 [1940-1990, d. 1960-2010 in Figure 5; and 40-yr periods, i.e. 1851-1890, 1891-1930, 1931-1970, 1971-2010 in](#)  
45 [Figure S11\), suggests an evolution of the SNAO fingerprint in time. The patterns observed in the early](#)  
46 [observational period \(1870-1920 and 1900-1950 in Figure 5a,b\) bear very strong resemblance to the one](#)

Monika Barcikowska 7/24/19 10:16 PM

**Deleted:** Similar results were obtained for the independent 40-yr periods (1851-1890, 1891-1930, 1931-1970, 1971-2010 in Figure S1). The EOF derived for periods before 1950s (shown here for



1 simulated in the CTRL run (Figure 4a), i.e. including the northern centers of action at southern Greenland and  
2 with the southern lobe located north of the Azores (~45°N, 35°E). In contrast, the EOF derived for the recent  
3 decades (e.g. 1960-2010 or 1971-2010) exhibits a weak northern lobe and a much stronger southern lobe, with  
4 the latter being also shifted north-east, towards the British Isles. These differences are also consistent with  
5 other observational analysis of the recent six decades (Blade et al. 2012 and Syed et al. 2012).

7 A similar evolution of the SNAO pattern is found in the 4 out of the 5 HIST members available when  
8 comparing the early observational periods with the most recent decades (Figure 5b,h; Figure SI2). For  
9 example, the pattern derived from all the HIST runs in the period 1870-1920 (Figure SI2, Figure 5b)  
10 resembles both the one derived from the observations (Figure 5a) and the one derived from the CTRL run  
11 (Figure 4a). In the most recent period (i.e.1960-2010, Figure SI2), the SNAO fingerprints simulated in HIST  
12 runs and the observed ones feature a much weaker northern lobe, and the southern lobe shifted north-eastward,  
13 towards the British Isles. This tendency intensifies even more when the more recent period is extended  
14 towards the future using PROJ members (e.g. 1970-2030, 1970-2060 Figure SI3). As the anthropogenic  
15 forcing is the only deterministic factor in the HIST and PROJ experiments, the above results highlight its  
16 potential importance in shaping the SNAO and hence explaining to some degree the temporal evolution of its  
17 spatial signature in the 20<sup>th</sup> century.

### 19 3.2.2 Impact of SNAO on the Mediterranean climate

21 The SNAO simulated in CM2.5 exerts an impact on the precipitation, surface temperature and geopotential  
22 height over the North Atlantic and Europe (Figure 4), which strongly resembles its observational counterpart  
23 (e.g. Folland et al. 2009, Blade et a. 2012). This includes a distinct tripolar pattern of precipitation anomalies  
24 with the lobe over southern Greenland, over northern Europe and its vicinity over the North Atlantic, and  
25 southern Europe (Figure 4c). The location corresponds closely with the fingerprint of anomalous surface  
26 temperature (Figure 4b).

28 The derived SNAO teleconnection at its positive (negative) phase, manifested in the positive (negative) SLP  
29 anomalies over its southern lobe (Figure 4a), is linked with an anomalous warming and drying (cooling,  
30 wetting) over northwestern Europe, and anomalous cooling and wetting (warming, drying) over the  
31 Mediterranean (Figure 4b,c). Consistent with the observations (Folland et al. 2009) the impact on the former  
32 region is almost twice as much stronger than on the latter, both in terms of precipitation and temperature. For  
33 example, the magnitude of correlation coefficients in the vicinity of the southern SNAO lobe (i.e. southwest  
34 of the British Isles) exceeds about 0.6 for precipitation and 0.5 for temperature, but in the Mediterranean, it  
35 remains below 0.35 and 0.4, respectively for precipitation and temperature.

37 The SNAO teleconnection to the northern and southern parts of Europe points also to different physical  
38 mechanisms. While the impact of the SNAO on northern Europe has been straightforwardly explained with  
39 changes in the North Atlantic storm tracks (Folland et al. 2009), the impact on the southern Europe  
40 hydroclimate (shown in observations by Linderholm et al. 2009) is manifest through the changes in the mid-  
41 and upper-tropospheric geopotential height. The correlation analysis between the SNAO time series and  
42 500hPa geopotential height (Figure 4b, contours), yields a tripolar structure, with the positions of the nodes  
43 being well collocated with those of precipitation and temperature. Hence, the negative correlations of  
44 geopotential height found over the Mediterranean provide a plausible explanation for the regional  
45 precipitation anomalies during the positive SNAO phase, which links to the local effects of anomalous mid-  
46 and upper tropospheric trough, associated cooling, and intensified potential instability over the Mediterranean.

Monika Barcikowska 8/23/19 6:06 AM  
Deleted: 5

Monika Barcikowska 8/19/19 8:04 AM  
Formatted: Not Highlight

Monika Barcikowska 8/19/19 8:04 AM  
Formatted: Not Highlight

Monika Barcikowska 8/23/19 5:30 AM  
Deleted: simulated

Monika Barcikowska 7/26/19 11:50 AM  
Deleted:

Monika Barcikowska 7/26/19 11:50 AM  
Deleted: and temperature

Monika Barcikowska 8/19/19 4:04 PM  
Deleted: the

Monika Barcikowska 8/19/19 4:05 PM  
Deleted: over

Monika Barcikowska 7/26/19 11:59 AM  
Deleted: and most of the Mediterranean region

Monika Barcikowska 8/23/19 6:08 AM  
Deleted: 5

Monika Barcikowska 8/23/19 6:08 AM  
Deleted: 5

Monika Barcikowska 8/23/19 6:08 AM  
Deleted: 5

Monika Barcikowska 7/26/19 3:05 PM  
Formatted: Not Highlight

Monika Barcikowska 7/26/19 10:45 AM  
Deleted: T

Monika Barcikowska 8/19/19 4:03 PM  
Deleted: the

Monika Barcikowska 7/26/19 3:05 PM  
Formatted: Font:12 pt

Monika Barcikowska 8/19/19 7:31 AM  
Formatted: Font:12 pt

Monika Barcikowska 8/19/19 8:04 AM  
Deleted: -

Monika Barcikowska 8/19/19 9:46 AM  
Formatted: Font:(Default) Times New Roman, 8 pt

### 3.3 Summer climate regime over the eastern Mediterranean

In this section, we investigate the ability of CM2.5 to simulate the key features shaping the hot and arid climate of the eastern Mediterranean (EMED, as defined in Sect. 2). This comprises a) the linkage between the surface and the mid- and upper-tropospheric dynamics, which maintains the thermal balance of the region; and b) the teleconnection with the Indian Summer Monsoon (hereafter ISM). Here we show results for July alone but those for June and August are shown as Supplementary Information. This choice is driven by the fact that the magnitude of subsidence and the Etesians is at its maximum in July while the response of the Rossby waves to monsoon rainfall is also strongest (Tyrlis et al. 2012, Lin et al. 2007, Lin et al. 2009).

The connection between the mid- and upper-tropospheric subsidence and surface circulation over EMED (Figure 6) is depicted with correlations between time series of the dominant EOF of vertical velocity ( $\omega$ ) at 500 hPa (i.e. EOF1 in Figure 6a) and geopotential height and wind vector at 850 hPa, outgoing longwave radiation and precipitation. The EOF pattern is almost identical to the simulated and observed climatology, featuring a monopole pattern being well collocated with the local maximum of subsidence in the vicinity of Crete (Tyrlis et al 2012, Ziv et al. 2004). The EOF persists as a dominant component up to the upper-troposphere (~200 hPa), explaining between 33% -35% of the total variance. Figure 6b,c shows that CM2.5 skillfully captures the connection between the strengthening mid- and upper-tropospheric subsidence and the intensifying Etesians, zonal pressure gradient and concomitant anticyclonic circulation in the central Mediterranean. Consistent with the impact of the adiabatic descent (and associated radiative cooling in dry regions under clear sky conditions), these changes are also manifest in the larger outgoing long-wave radiation and to a smaller degree in reduced precipitation (Figure 6e,f). The simulated in CM2.5 relationship closely resembles its observational counterpart, derived by correlating the regional anomalies of  $\omega$  500hPa and meridional wind using the detrended NCEP–DOE data set, shown in Figure 6d. Note that due to a relatively short data set (1979-2015), the correlations are not significant at the 10% level for some regions and thus not shown, even if they agree well with those simulated, for example, the positive correlations in northwest Africa.

The correlations derived between the  $\omega$  and monsoon indices (Figure 6) suggest that the model reproduces the impacts of the Indian summer monsoon teleconnection, consistent with the previous modeling and observational studies (Hoskins et al. 1996, Hoskins et al. 2001, Tyrlis et al. 2012, Ziv 2004, Cherchi et al. 2014). The analysis represents the linkage between the strengthening subsidence over the EMED region and the intensified Indian summer monsoon, represented here with the negative anomalies of the OLR, positive anomalies of precipitation and vertically integrated water vapor (not shown) centered over the northwestern coast of India. The depicted intensification of the monsoon is also in congruence with the intensified heat low over the Arabian Peninsula and the Arabian Sea, and the intensified south-westerlies over the Arabian Sea, which feed the monsoon with moisture (Figure 6b, c). As pointed previously in Ziv et al. 2004, the linkage exerts also an effect on the EMED surface circulation by modulating the intensity of the heat low and hence the intensity of the zonal pressure gradient over the Mediterranean and associated regional northerly flow, i.e. Etesians.

These results suggest that CM2.5 is capable of capturing the most prominent features of the summer climate regime over the EMED. Changes in the existing local relationships may influence the regional temperature regime. Accordingly, the next section investigates the projected future Mediterranean climate, interpreting this through the prism of the governing factors, i.e. large-scale circulation, local relationships and teleconnections.

Monika Barcikowska 8/1/19 3:05 PM

Formatted: Justified

Monika Barcikowska 8/3/19 10:30 PM

Deleted: his ...ection, we investigate ... [3]

Monika Barcikowska 8/1/19 5:07 PM

Deleted: -

... [4]

Monika Barcikowska 8/1/19 2:57 PM

Formatted: Font:12 pt

Monika Barcikowska 8/19/19 10:25 AM

Formatted

... [5]

Monika Barcikowska 7/31/19 9:37 PM

Deleted: -

Monika Barcikowska 8/1/19 3:48 PM

Formatted: Font:(Default) Times New Roman

Monika Barcikowska 8/1/19 5:09 PM

Deleted: : the mid- and upper tropospheric subsidence over the EMED and the low-level Etesian winds. Moreover, these results also show that the model reproduces their links with the I...SM... Changes in the existi ... [6]

Monika Barcikowska 8/1/19 5:17 PM

Deleted: -

1 | **4. Climate changes in the 21<sup>st</sup> century,**  
2 | **4.1 Comparison of future and present summer climate**

3  
4 | CM2.5 projections of future large-scale circulation over the Euro-Atlantic region are largely consistent with  
5 | those seen in the CMIP3 and CMIP5 simulations. The most prominent feature of the derived changes is a  
6 | northward shift and strengthening of the North Atlantic meridional SLP gradient. This pattern, manifest as an  
7 | SLP dipole with cyclonic anomalies centered over Greenland and anticyclonic anomalies centered southwest  
8 | of the British Isles, is a typical fingerprint of anthropogenic climate change (Collins et al. 2013). The  
9 | anthropogenic fingerprint closely resembles the CTRL-based SNAO at its positive phase (despite a slight shift  
10 | northeast of the CTRL SNAO), thereby suggesting a possible contribution of the anthropogenic component  
11 | towards positive tendencies of the future SNAO, quite like as found by Folland et al. 2009 for HadCM3 and  
12 | HadGEM1.

13  
14 | Figure 7 indicates a very strong warming reaching locally 7°C, and an intensification of the thermal low over  
15 | the Sahara, the eastern Mediterranean and the Arabian Peninsula. The local hot spot of the warming, located  
16 | over the Levant and inland Arabian Peninsula, collocates well with an anomaly of convergent flow and  
17 | ascending air, expanding from the surface up to mid-tropospheric levels (Figure 2c, Figure SI4), and thereby  
18 | intensifying the Persian trough. The latter contributes to the weaker subsidence in the eastern Mediterranean  
19 | and, together with an intensified subsidence over the central Mediterranean, shifts the local maximum of  
20 | subsidence towards the northwest.

21  
22 | The projected changes in the circulation over Europe show important differences from the CMIP5 multi-  
23 | model ensemble of RCP8.5 scenario (Collins et al. 2013) and the CMIP3 ensemble of the A1B scenario  
24 | (Giorgi and Lionello 2008), both in quantitative and qualitative terms. The changes simulated in CM2.5 can  
25 | be largely described as a transition zone between the intensifying anticyclonic circulation, centered in the  
26 | vicinity of British Isles, and intensifying thermal low over the eastern Mediterranean and the Middle East.  
27 | Hence the northwestern and central parts, including the central Mediterranean feature an increase in SLP.  
28 | Both, the increasing SLP in the central Mediterranean and the decreasing SLP in the eastern Mediterranean  
29 | amplify the zonal pressure gradient in this region and the concomitant Etesian winds. In contrast, CMIP5  
30 | ensemble indicating a decrease in SLP for almost the entire Europe (except the British Isles), and this exerts a  
31 | weakening effect on the regional zonal pressure gradient and the associated northerly flow (Collins et al. 2013,  
32 | Fig 12.18).

33  
34 | The warming projected in CM2.5 shows a stark gradient between the southwestern and northeastern parts of  
35 | Europe, which is consistent with the CMIP5 and the EURO-CORDEX ensembles. However, for the latter, the  
36 | gradient is weaker and the minimum of warming shifted northward (see Fussel et al. 2017, Map3.4; Figure  
37 | SI6), i.e. located over the southeastern Baltic countries. In CM2.5 the minimum of warming is located in the  
38 | northern Balkans and southeast Europe, in the vicinity of the Black Sea coast (Figure 7b), indicating values  
39 | falling within 0.5-2.5°C and accompanied also with wetting tendencies. The regions such as the Iberian  
40 | Peninsula, southern Balkans and Asia Minor feature warming between 3.5 and 6°C. The maximum of  
41 | warming is located over North Africa and Levant, with values falling within the range of 5-8°C.

42  
43 | CM2.5 features (Figure 7c) a sharp transition zone between the drying in southwestern Europe and the wetting  
44 | in northeastern Europe. However the gradient in CM2.5, analogously to the temperature changes gradient, is  
45 | much sharper and the wetting tendencies extend southward (down to northern Balkans) when compared with  
46 | the CMIP3 and CMIP5 ensemble (Fussel et al. 2017, Map 3.8). Owing to its relatively high resolution, CM2.5

Monika Barcikowska 8/19/19 10:29 AM  
**Deleted:** -

Monika Barcikowska 8/1/19 9:00 PM  
**Deleted:** In CM2.5, the projected cha... [7]

Monika Barcikowska 8/1/19 9:07 PM  
**Deleted:** to a large extent to...ith thos... [8]

Monika Barcikowska 8/2/19 1:26 PM  
**Formatted:** Font:8 pt

Monika Barcikowska 8/1/19 9:06 PM  
**Formatted:** Font:8 pt

Monika Barcikowska 8/1/19 9:18 PM  
**Deleted:** The most prominent feature over the Euro-Atlantic region, a...orthward... [9]

Monika Barcikowska 8/1/19 9:36 PM  
**Formatted:** Font:(Default) Times New Roman

Monika Barcikowska 8/2/19 2:02 PM  
**Deleted:** CM2.5...igure 7 projection... [10]

Monika Barcikowska 8/2/19 2:38 PM  
**Formatted:** ... [11]

Monika Barcikowska 8/2/19 4:02 PM  
**Deleted:** -

Monika Barcikowska 8/2/19 5:59 PM  
**Deleted:** The project...how importa... [12]

Monika Barcikowska 8/2/19 7:07 PM  
**Formatted:** Font:12 pt

Monika Barcikowska 8/2/19 10:11 PM  
**Deleted:** Hence the latter contributes in CM2.5 to a stark contrast in the warming between the Mediterranean coast including coastal region of Balkans (4-6°), and the inland Balkans together with southeastern Europe (1°C). This temperature gradient

Monika Barcikowska 8/2/19 9:51 PM  
**Formatted:** Font:8 pt

Monika Barcikowska 8/2/19 3:19 PM  
**Deleted:** ...Figure 79...b... a sharp... [13]

1 | also provides more spatially refined information, which includes, for example, sharper gradients along the  
2 | coasts or in the mountainous regions. All coastal regions experience reductions in precipitation, expected from  
3 | the strengthening temperature contrast between the fast warming land and slower warming sea. These  
4 | reductions are especially pronounced along the northwestern coasts of the Iberian Peninsula, where rainfall is  
5 | typically larger due to incoming North Atlantic storms.

Monika Barcikowska 8/15/19 1:09 PM  
Deleted: ...these reductions are espd ... [14]

## 4.2 Future changes in SNAO-Mediterranean teleconnections

9 | Analysis of the 20<sup>th</sup> and 21<sup>st</sup> century simulations exhibits long-term changes in the behavior of the SNAO,  
10 | both in terms of magnitude and pattern. The temporal evolution of the SNAO, depicted as an ensemble  
11 | average of the HIST+PROJ runs (Figure 8c), indicates its positive tendencies both in the latter half of the 20<sup>th</sup>  
12 | century and the 21<sup>st</sup> century. However, the trend found for the former period is much weaker and in separate  
13 | realizations is even hampered by relatively strong interannual- to multi-decadal variations. This is consistent  
14 | with the SNAO signal observed in the recent decades, which features rich variability across time scales and a  
15 | relatively weak positive trend, as described in section 3.2.1. For the latter period (particularly 2040-2100) the  
16 | trend becomes strong enough to be discernible in every realization.

Monika Barcikowska 8/6/19 11:32 AM  
Formatted ... [15]

Monika Barcikowska 8/6/19 11:34 AM  
Deleted: depicted (Figure 10c) ...he ... [16]

Monika Barcikowska 8/6/19 11:49 AM  
Formatted: Superscript

18 | Further analysis points to the subtle changes in the future spatial pattern of the SNAO. Comparison of the SLP  
19 | fingerprint between 1960-2010 and 2050-2100 (Figure 8a,b) indicates a northeastward shift, thereby making  
20 | the southern lobe of the SNAO located closer to the British Isles. This feature is also consistent with the  
21 | projected intensification and northeastward shift of the meridional SLP gradient over the North Atlantic  
22 | (Figure 7a). The future changes in the SNAO are also discernible in the teleconnection with the European  
23 | hydroclimate. The comparison of the correlations, derived for the time series of the SNAO component and  
24 | precipitation anomalies, (Figure 8a,b) indicates a strengthening impact over Europe, i.e. enhanced drying  
25 | (wetting) in northern Europe and wetting (drying) over southern Europe during the positive (negative) SNAO  
26 | phase. The changes over the Mediterranean are found mostly over the Iberian Peninsula, southern Balkans and  
27 | Asia Minor, suggesting that the future intensification of the SNAO may play in these regions an important  
28 | role in moistening and offsetting the drying effects of the anthropogenic changes.

Monika Barcikowska 8/7/19 8:42 AM  
Deleted: suggests...the also ...ubtle ... [17]

30 | As shown in the previous section, changes in the seasonal precipitation over the Mediterranean (Figure 7b,c),  
31 | indicate strong warming and drying. Hence the key implication of these results is that without the SNAO the  
32 | future climate drying in the Mediterranean would be even more severe. Figure 8d,e depicts the seasonal  
33 | regional future changes (1961-1999 versus 2061-2099), and the changes without the contribution of the  
34 | SNAO, that offsets the regional drying. The comparison of the changes indicates that the largest differences  
35 | are well collocated with the location of the intensified impact of the SNAO (Figure 8a,b). For example, the  
36 | average drying would intensify from ~-0.4 to -0.65 mm/day for the southeast and central Iberian Peninsula,  
37 | from ~-0.3 to -0.55mm/day over the Balkan coast, and from ~-0.6 to -0.8 mm/day for parts of Asia Minor,  
38 | when the impact of the SNAO is removed. These differences underline the role of the SNAO in shaping the  
39 | climate of southern Europe.

Monika Barcikowska 8/7/19 12:36 PM  
Deleted: It is important to mention t ... [18]

Monika Barcikowska 8/9/19 7:42 AM  
Deleted: other aspects of

Monika Barcikowska 8/19/19 10:52 AM  
Formatted: Not Highlight

Monika Barcikowska 8/9/19 7:42 AM  
Deleted: climate

Monika Barcikowska 8/19/19 10:52 AM  
Formatted: Not Highlight

Monika Barcikowska 8/9/19 7:42 AM  
Deleted: in

Monika Barcikowska 8/19/19 10:52 AM  
Formatted: Not Highlight

Monika Barcikowska 8/9/19 7:42 AM  
Deleted: in

Monika Barcikowska 8/19/19 10:52 AM  
Formatted: Not Highlight

Monika Barcikowska 8/19/19 10:45 AM  
Deleted: EMED...region ... [19]

Monika Barcikowska 8/9/19 8:02 AM  
Deleted: investigates other ... [20]

## 4.3 Future changes in the summer regime of the eastern Mediterranean

43 | This section focuses on future changes in the key local features shaping the regime of the EMED climate. This  
44 | includes an analysis of the stationarity of the local linkage between the low- and mid-to-upper tropospheric  
45 | dynamics and the influence of the local surface warming on the surface circulation.



### 4.3.1 Changes in the local linkage shaping the EMED climate regime

Figure 9 compares the HIST and the PROJ five-member ensemble average of the correlations, derived between the regional mid-tropospheric subsidence and the indices of the surface circulation. The comparison of the correlations, which represent the dynamical linkage governing the present and future climate regime over EMED, exhibits qualitative and quantitative differences. For the future period the correlations, estimated for both, the regional surface pressure systems (Figure 9b), the concomitant zonal pressure gradient and the surface northerlies (i.e. Etesians, Figure 9d), are substantially weaker, e.g. by more than a factor of two (from  $\sim 0.7$  to  $\sim 0.3$ ) for the regions of Levant and Persian Gulf. Figure 9c,d also shows that for some regions of North Africa the linkage almost vanishes. This is consistent with the radically reduced correlations estimated for the water vapour and precipitation (from  $\sim 0.4$ - $0.5$  to  $\sim 0$ ) over the African monsoon region (Figure 9e,f), which largely depends on the influx of moisture transported with the northerly flow over EMED and North Africa.

On the other hand, correlations between the EMED subsidence and ISM indices (July), i.e. precipitation and column-integrated water vapour (Figure 9e,f), do not show quantitative differences. The patterns, derived for both variables are slightly shifted towards the southwest in the future period, which is consistent with the changes in the atmospheric circulation, supplying the ISM monsoon with moisture.

These results do suggest a pronounced weakening of the local linkage between the mid- and upper-tropospheric subsidence and surface circulation over the EMED. Moreover, given that the local linkage serves as a “medium path” for the teleconnection between the ISM and surface circulation over EMED, future weakening of the local linkage will most likely diminish the impact of this teleconnection on the EMED surface circulation. On the other hand, the projected intensification of the heat low over EMED, North Africa, and the Middle East points to an increasing role of the warming over the arid surfaces. Thus, in the following section, we explore apparent nonlinearities in the summer climate regime of the eastern Mediterranean associated with the local surface temperature.

### 4.3.2 Nonlinear dependency of the local linkages between the low-tropospheric and the mid-tropospheric dynamics and their contributions to the thermal balance over EMED.

In this section, we focus on the impacts of the warming local surface temperature on the low-level circulation, including the linkage between the low-level and the mid-tropospheric dynamics over EMED. The analysis uses the CTRL run, which excludes the time-varying anthropogenic climate forcing and hence allows us to focus on the natural variability of the system and nonlinear interactions that would be difficult to statistically calculate in shorter HIST runs. As described in section 2, we analyze two samples with 300 cases of the lowest and highest monthly mean temperature in July, with respect to the mean surface temperature over the EMED region.

The following analysis compares the strength of the local linkage between the mid- and upper-tropospheric subsidence over EMED, derived for the sample with the cold and warm temperatures, much as done in the previous section comparing recent historical and future periods. The comparison, consistent with the results shown in previous section (Figure 9), indicates a radical weakening of the linkage derived between the mid-level subsidence over EMED and the zonal surface pressure systems over the central and eastern Mediterranean, Etesian winds and their extension over North Africa and the Persian Gulf, and precipitation over the Sahel (Figure S16).

Monika Barcikowska 8/19/19 10:51 AM

**Deleted:** The projected future intensification of the Etesians as well as the weakening subsidence should yield a cooling and wetting effect on that region. Nevertheless, future projections indicate a very strong warming and drying in this region. This suggests a decreasing influence of the atmospheric dynamics on the temperature balance of this region and an increasing impact of surface warming on surface circulation. The latter is manifested in the intensification of the heat low over Sahara, EMED and Arabian Peninsula, accompanied by anomalous surface convergence and ascending air centered over the maximum warming—the Levant and the Arabian Peninsula. ... [21]

Monika Barcikowska 8/9/19 8:19 AM

**Formatted:** ... [22]

Monika Barcikowska 8/9/19 3:38 PM

**Deleted: and...remote relationship...** ... [23]

Monika Barcikowska 8/9/19 9:08 AM

**Deleted:** Figure 11 compares the HIST and PROJ five-member ...ensemble averag... [24]

Monika Barcikowska 8/9/19 10:09 AM

**Deleted:** At the same time...n the ot... [25]

Monika Barcikowska 8/9/19 10:28 AM

**Deleted:** imply generally insignificant changes in the future mid- or upper-tropospheric teleconnection between the EMED and ISM regions. However the... [26]

Monika Barcikowska 8/15/19 1:09 PM

**Deleted:** ...

Monika Barcikowska 8/9/19 4:38 PM

**Deleted: interrelations**

Monika Barcikowska 8/9/19 5:06 PM

**Deleted:** e nonlinear dynamical influences over EMED can be ... analysis uses ex... [27]

Monika Barcikowska 8/9/19 6:14 PM

**Deleted:** We carry out a correlation analysis for these two periods, much as done in the previous section comparing recent historical and future periods. Figure S1 shows a radical drop in derived correlations between the mid-level subsidence and the Mediterranean pressure, Etesian winds and their extension over the North Africa and Persian Gulf, and water vapor over the Sahel. These results are similar to those comparing present and future climate for these variables (Fig 11). ...

Monika Barcikowska 8/9/19 5:06 PM

**Formatted:** Font:(Default) Times New Roman



1 | Figure 10 depicts a direct response of the summer Mediterranean climate to the surface warming over EMED,  
2 | estimated with composite differences between the two samples (high temperature minus low temperature), in  
3 | terms of temperature, relative humidity, pressure and wind vector, geopotential height at 500 hPa and 800 hPa,  
4 | omega at 500 hPa and precipitation. Figure 10c features bipolar SLP anomalies, with low-pressure anomaly  
5 | over North Africa, EMED and the Middle East, and an anomalous anticyclonic circulation between northeast  
6 | and northwest of this region. While the former is well collocated with the intensified heat low anomalies  
7 | found as an anthropogenic signal (Figure 7a), the latter is centered over the Black Sea and spreads towards the  
8 | central Mediterranean, creating a stronger zonal pressure gradient over the Mediterranean and intensified  
9 | Etesian winds. The intensified heat low over the EMED and Arabian Peninsula (Figure 10c) is also consistent  
10 | with the enhanced local convergence and reduced subsidence at the low- and mid-tropospheric levels at 500  
11 | hPa (Figure 10e) and 700 hPa (not shown). At the same time, the positive SLP anomalies (Figure 10c) and the  
12 | increased subsidence over Asia Minor and the Black Sea are physically consistent with increased adiabatic  
13 | warming and stability, manifest in the local maximum warming, reduced relative humidity and precipitation.  
14 | The analysis repeated for the July-August season yields similar results, although with a reduced magnitude  
15 | due to a weaker signal in June and August (Figure SI7).

Monika Barcikowska 8/23/19 6:23 AM  
Deleted: 2... depicts a direct respons... [28]

Monika Barcikowska 8/23/19 6:23 AM  
Deleted: 2... features shows... bipolar... [29]

Monika Barcikowska 8/9/19 6:25 PM  
Formatted: Font:10 pt

16 |  
17 | The analysis repeated for the response to the warming over the domains extended towards southern parts of  
18 | the central and western Mediterranean (Figure SI8a,b) yields qualitatively similar results (i.e. the bipolar SLP  
19 | anomalies), but with an increased magnitude of the response over the southwestern Mediterranean. On the  
20 | other hand, analysis repeated for the warming regions confined to the Levant, Arabian Peninsula and Asia  
21 | Minor and Black Sea (30°-50°E, 30°-45°N, Figure SI8e), shows the pattern with the response (anticyclone  
22 | anomaly) intensified towards the Middle East. The most similar results are obtained, qualitatively and  
23 | quantitatively, when the region is confined to the same latitudes but slightly extended towards east and west  
24 | (30°-50°E, 30°-36°N, Figure SI8c), i.e. centered over the Levant and northern parts of Arabian Peninsula.

Monika Barcikowska 8/9/19 6:28 PM  
Formatted: Font:(Default) Times New Roman

Monika Barcikowska 8/10/19 6:16 AM  
Deleted: A...alysis repeated for of... [30]

25 |  
26 | The derived composite response to the warming over EMED is manifest in the local surface circulation. The  
27 | resulting bipolar SLP anomaly leads to the intensified zonal pressure gradient and the concomitant Etesians  
28 | over the central-eastern Mediterranean. The positive SLP anomalies, centered over the central and  
29 | northeastern parts of the Mediterranean are consistent with the increased subsidence and drying in these  
30 | regions (i.e. Italy, the Balkan coast and Asia Minor). The intensified heat low over the EMED and associated  
31 | anomalous convergence weaken the low- and mid-tropospheric subsidence over the EMED and the Arabian  
32 | Peninsula. All these responses are consistent with the future changes projected in JJA (Figure 7a,b,c, Figure  
33 | SI4a,c,e), and particularly in the month of July (Figure SI4b,d,f), suggesting an important role of the warming  
34 | arid regions of Levant and Arabian Peninsula in the future climate regime of the eastern Mediterranean.

Monika Barcikowska 8/10/19 7:09 AM  
Formatted

Monika Barcikowska 8/10/19 7:15 AM  
Deleted: anomalous...warming over... [32]

35 |  
36 | This analysis indicates that the dynamical regime over the EMED has a nonlinear influence on local  
37 | temperature. During relatively cool years the dynamical relationship between the low-level circulation and  
38 | mid-level subsidence, which balances the temperature over EMED, seems to be much stronger. By contrast,  
39 | warming over the EMED region can trigger a local response in the surface atmospheric circulation, which  
40 | weakens the local dynamical linkages and hence their contribution in maintaining the local temperature  
41 | balance. Hence it is possible that surface temperature-driven atmospheric responses will become a more  
42 | prominent factor shaping future Mediterranean climate. This idea is supported by the consistency of this  
43 | response (i.e. strong warming, intensifying heat low, anomalous convergence and very pronounced ascending  
44 | motion at the low and mid-levels of the EMED and Arabian Peninsula, intensified zonal pressure gradient and  
45 | Etesians, drying over Asia Minor and southern Balkans) with projected anthropogenic changes over the

Monika Barcikowska 8/10/19 7:41 AM  
Deleted: warming and drying over Asia Minor...

Monika Barcikowska 8/10/19 7:37 AM  
Formatted: Font:(Default) Times New Roman

1 EMED region. Similar results are obtained for June and August, although with slightly lower intensity and  
2 location of the SLP and precipitation anomalies (not shown).  
3

Monika Barcikowska 8/19/19 10:57 AM  
**Deleted:** different

4 The analysis, however, does not explain the processes involved in the dipole-like response in the circulation,  
5 which comprises SLP, winds and omega anomalies north from the EMED region (particularly Asia Minor and  
6 the Black Sea). One might suspect that, in response to warming over the EMED, the anomalous convergence  
7 and ascending motion over the EMED triggers a seesaw connection with northward-located regions. This link  
8 could stem from the interactions of the anomalous warming and upward velocity anomalies with the  
9 seasonally varying descending branch of the Hadley cell over EMED, in result expanding it towards Asia  
10 Minor. Testing this hypothesis needs more elaborate analysis and could be the objective of future research.  
11

Monika Barcikowska 8/19/19 11:00 AM  
**Deleted:** includes

Monika Barcikowska 8/21/19 3:59 PM  
**Deleted:** coming

## 12 5. Summary and Discussion

13  
14 Based on the state of the art future projections (CMIP3 and CMIP5-generation) the Mediterranean has been  
15 identified as a climate change hot spot (Giorgi and Lionello 2008), not only due to the sensitivity of its climate  
16 to the anthropogenic forcing but also due to the socio-economic vulnerability of the local societies. Yet the  
17 projected changes are not fully reflected in the observations for the second half of the 20<sup>th</sup> century. While the  
18 derived anthropogenic fingerprint suggests strong warming and drying during the summer, the observations  
19 indicate opposite wetting tendencies for some regions—in the vicinity of Black Sea and off the Balkan coast.  
20 This discrepancy may stem from the fact that the Mediterranean climate features abundant cross-scale  
21 variations, which at present dominate the anthropogenic signal. But there can be other reasons for this  
22 inconsistency, i.e. the deficiencies in models' representation of land-atmospheric feedbacks (as mentioned  
23 above) or the deficiencies in capturing impacts of certain teleconnections. The former has been shown to  
24 cause an overestimation of the projected future summer warming and drying in most of CMIP3 and CMIP5  
25 models (Christensen and Boberg, 2012, Christensen and Boberg, 2012, Mueller and Seneviratne, 2014),  
26 particularly in the Mediterranean, Central and Southeast Europe (Diffenbaugh et al. 2007, Hirschi et al. 2011,  
27 Seneviratne et al., 2006). The latter has been suggested to incapacitate CMIP3/CMIP5 models in offsetting  
28 projected future regional drying, and hence to spuriously exaggerate the regional warming and drying (Blade  
29 et al. 2012). Obtaining realistic future projections for this region requires not only refined spatial scales, but  
30 also a realistic balance between the contributing impacts of local land-atmosphere feedbacks, large-scale  
31 circulation, and teleconnections. In this study, we use the high-resolution CM2.5 climate model integrations to  
32 analyze the projected future changes in temperature and precipitation over the Mediterranean and discern  
33 between the role of the simulated SNAO teleconnections, and the local impacts of warming land surface and  
34 associated land surface –air interactions.  
35

Monika Barcikowska 7/26/19 5:12 PM  
**Deleted:** -

Monika Barcikowska 8/21/19 5:18 AM  
**Deleted:** The

Monika Barcikowska 7/29/19 1:51 PM  
**Deleted:** . The model very accurately reproduces key regional features of the associated large –scale atmospheric circulation, both in terms of the location and magnitude. This includes, for example, the subtropical mid-tropospheric anticyclone between the Levant and South Asia, and the low-tropospheric zonal pressure gradient between the subtropical North Atlantic anticyclone and the massive Asian monsoon heat low. The spatial resolution of the integrations allows for capturing the of the low-level atmospheric ,branchover the Aegean Sea and its southward extension toward the Sahel region, as well as over the Persian Gulf.

36 Our analysis demonstrates the high ability of the CM2.5 model in reproducing key large-scale and regional  
37 features shaping the complex summer Mediterranean climate thereby highlighting advantages of employed  
38 high spatial-resolution. The model accurately captures spatial features and magnitude of the subtropical mid-  
39 tropospheric anticyclone extended between the Levant and South Asia, as well as the low-tropospheric zonal  
40 pressure gradient between the subtropical North Atlantic anticyclone and the massive Asian monsoon heat  
41 low. The pressure gradient, manifested in the Mediterranean as a complex structure of northerly winds, i.e.  
42 Etesians, is resolved in the model with great detail including the distinguishable branch over the Aegean Sea  
43 and its southward extension toward the Sahel region, as well as the one over the Persian Gulf. The mean  
44 precipitation, which features an exceptional spatial complexity in the Mediterranean, is represented with a  
45 much higher degree of realism when compared with the low-resolution CM2.1, for example.  
46

1 Furthermore, we find that CM2.5 faithfully reproduces the most prominent pattern of atmospheric variability  
2 over the North Atlantic, i.e. the North Atlantic oscillation, and its impact on the Mediterranean hydroclimate.  
3 In the simulations and observations, SNAO emerges as a leading EOF component, explaining ~34% and  
4 ~28% of the total variance over the analysis domain, respectively (Folland et al. 2009). Remarkably, the  
5 simulated pattern corresponds better to the observed one before the 1970s, rather than for the more recent  
6 decades. Moreover, the simulated impact of the SNAO on the Mediterranean hydroclimate is more consistent  
7 with the century-long observations (1900-1998, 1900-2007, in Folland et al. 2009), rather than the most recent  
8 decades of observations (1950-2010 in Blade et al. 2012). For example, the impact on precipitation and  
9 surface temperature derived with the shorter data set is relatively high (with the magnitude of correlations  
10 reaches up to 0.5-0.6), but with the significant results confined mostly to the Balkans and Italy. In contrast, the  
11 correlations derived for the century-long precipitation record are of lower magnitude (i.e. lower than 0.45),  
12 but they are significant over most parts of the Mediterranean, as shown in Folland et al. 2009. The study,  
13 mentioned above, explains also that the impact of SNAO is to some extent shaped by its low-frequency  
14 variations that may have partly originated from anthropogenic forcing. This forcing contributes to a smaller  
15 extent in the observational record before the 1950s and is also not included in the CM2.5 control run. Hence,  
16 the apparent ambiguity of the observed SNAO impacts may stem from the varying in time importance of the  
17 low-frequency and high-frequency factors which shape the SNAO in the 20<sup>th</sup> century (as highlighted by  
18 Linderholm and Folland 2017), though this issue still requires further investigation. Further analysis of the  
19 CM2.5 runs shows also that the impacts of the SNAO teleconnection on the Mediterranean precipitation are  
20 comparable with those simulated with the previous generation model, such as HADCM3 (Blade et al. 2012).  
21 The impacts simulated with CM2.5 are also indistinguishably different from those captured in the GFDL  
22 CM2.1 runs (i.e. the low-resolution predecessor of CM2.5), except the region of Asia Minor, where CM2.1  
23 does not capture the significant impact of SNAO.

25 Moreover, the model skillfully captures the linkage between the low-level northerly flow and the mid- and  
26 upper-tropospheric subsidence over the eastern Mediterranean. These two factors have counteracting effects  
27 on the regional temperature, hence playing an important role in maintaining the local temperature balance.  
28 Therefore, their linkage is the key feature that shapes the summer climate for the eastern Mediterranean.  
29 Additionally, the derived correlations between the mid- and upper tropospheric subsidence over the  
30 Mediterranean, and the indices of the Indian summer monsoon are consistent with the monsoon-desert  
31 mechanism (Rodwell and Hoskins, 1996, and Tyrlis et al., 2013).

33 Overall, our analysis of the CM2.5 control run confirms the capability of the model to simulate key  
34 components of the regional climate, in particular the SNAO teleconnection, and the local linkage between the  
35 surface and upper-level dynamics in the Mediterranean summer regime. This allowed us to further investigate  
36 the regional future changes through the prism of the evolution of these two factors.

38 The CM2.5 projections of large-scale climate changes over the Euro-Atlantic region are largely consistent  
39 with the CMIP5 ensemble projections. The projected changes in large-scale circulation, i.e. the expansion of  
40 the Hadley cell, and the intensification and northward shift of the atmospheric meridional cells, constitute a  
41 typical anthropogenic fingerprint of the future changes over the North Atlantic (e.g. Collins et al. 2013,  
42 Folland 2009). Consistent with the previous CMIP projections (e.g. Collins et al. 2013, Folland 2009), these  
43 changes are reflected in the strengthening of the SNAO towards its positive phase. For Europe, CM2.5  
44 projects drying over the subtropics (southern Mediterranean) and wetting of the mid-latitudes (northern  
45 Europe), which is consistent with the previous generations of the models, and explained with the “wet-get-  
46 wetter and dry-get-drier” mechanism (Held and Soden, 2006; Seager et al., 2007).

Monika Barcikowska 8/21/19 5:19 AM  
Deleted: Our analysis shows...urthe... [33]

Monika Barcikowska 8/16/19 3:47 PM  
Formatted: Superscript

Monika Barcikowska 8/21/19 7:41 AM  
Deleted: the

Monika Barcikowska 8/16/19 4:20 PM  
Deleted: CM2.5...to simulate key... [34]

Monika Barcikowska 8/16/19 4:20 PM  
Formatted: Not Highlight

Monika Barcikowska 8/16/19 4:20 PM  
Formatted: Not Highlight

Monika Barcikowska 8/21/19 5:56 AM  
Deleted: ns

Monika Barcikowska 8/16/19 4:20 PM  
Formatted: Not Highlight

Monika Barcikowska 8/16/19 4:20 PM  
Formatted: Not Highlight

Monika Barcikowska 8/21/19 5:54 AM  
Deleted: e

Monika Barcikowska 8/16/19 4:20 PM  
Formatted

Monika Barcikowska 8/21/19 5:55 AM  
Deleted: analysis...investigates...th... [36]

Monika Barcikowska 8/16/19 4:20 PM  
Formatted: Not Highlight

Monika Barcikowska 8/16/19 4:20 PM  
Deleted: -

Monika Barcikowska 8/2/19 7:40 PM  
Formatted: Font:8 pt

Monika Barcikowska 8/21/19 5:59 AM  
Deleted: he analysis of t...e CM2.5... [37]

Monika Barcikowska 8/14/19 10:17 AM  
Formatted: Font:12 pt

Monika Barcikowska 8/14/19 10:18 AM  
Deleted: In ...M2.5 projects...the g... [38]

Monika Barcikowska 8/14/19 10:24 AM  
Formatted: Highlight

1 Nonetheless, the CM2.5 projections show distinguishable differences in the large-scale atmospheric  
2 circulation patterns of the future changes and a higher complexity of the derived temperature and precipitation  
3 changes over Europe, when compared with the CMIP3 and CMIP5 ensembles. Importantly, CM2.5  
4 simulations imply less radical magnitudes of the warming over most of Europe, fewer regions and smaller  
5 magnitudes of drying anomalies, as well as larger areas with wetting anomalies. For example, the CMIP  
6 ensembles feature negative SLP tendencies over most of Eurasia, including an intensification of the heat low  
7 over the Mediterranean, as contrasted with the CM2.5 projections featuring negative SLP tendencies over the  
8 Mediterranean and the positive SLP tendencies over western and central Europe. As a consequence, the  
9 former indicates rather a weakening of the atmospheric circulation over the Mediterranean, while the latter  
10 indicates a strengthening zonal SLP gradient and hence stronger northerly flow, i.e. Etesian winds, in this  
11 region.

Monika Barcikowska 8/16/19 4:32 PM  
Deleted: However,...he CM2.5 proj... [39]

12  
13 Regarding the precipitation changes, CM2.5 simulates a sharp gradient between drying over southwest Europe,  
14 including most of the Mediterranean, and wetting over northeast and central Europe, including the Alps and  
15 northern parts of Balkans. This feature distinguishes the CM2.5 from the previous CMIP runs, which project  
16 mostly a strong drying over whole Europe, except Scandinavia, as depicted for example in the CSIRO-Mk3-6-  
17 0 model ensemble (Figure SI5).

18  
19 Consistent with the previous CMIP ensembles, CM2.5 also projects a strong gradient between warming in  
20 southwestern Europe and weaker warming in northeastern Europe. For example, the warming over the Iberian  
21 Peninsula, southern Balkans and Alps reaches locally 6°C, and the warming over the North African coast and  
22 the inland Levant region exceeds locally 7°C. The warming over northern and central parts of the region (i.e.  
23 southern France and in Italy) is slightly lower and reaches locally up to 4.5-5°C.

Monika Barcikowska 8/19/19 11:02 AM  
Formatted [40]

24  
25 However, the warming projected in CM2.5 (Fig 7b,c) is much less radical, when compared to the CMIP3  
26 (Dubrowski et al. 2014) and CMIP5 (Collins et al. 2013) ensembles, as well as the high resolution EURO-  
27 CORDEX GCM-RCM RCP8.5 multi-model ensemble (Fussel et al. 2017, Jacob et al. 2014, Figure SI5). This  
28 discrepancy is distinguishable in particular for the northern Balkans and southeastern Europe. There, CM2.5  
29 shows a minimum warming of 0.5-2.5°C. In contrast, the 10-member RCP8.5 ensemble of the CSIRO-Mk3-6-  
30 0 model indicates warming exceeding 6°C for these regions (Figure SI5) and the multi-model ensemble  
31 average of combined GCM-RCM simulations from the EURO-CORDEX initiative (Fussel et al. 2017, Map  
32 3.4, pp. 76) indicates warming of 3.5 - 5.5°C.

Monika Barcikowska 8/19/19 11:02 AM  
Formatted [41]

33  
34 The very intense warming and drying over Europe projected in the CMIP ensembles has been linked to a  
35 temperature-dependent warm summertime bias, caused by deficient representations of moisture-temperature  
36 feedbacks in most of CMIP3 and CMIP5 models (Christensen and Boberg, 2012; Mueller and Seneviratne,  
37 2014, Boberg and Christensen, 2012). On the other hand, Berg et al. 2016; Milly et al. 2014 demonstrated that  
38 the representation of soil moisture and land-atmospheric feedbacks between soil moisture and precipitation in  
39 the LM3 model, used in CM2.5, is significantly improved. Moreover, the atmosphere-land interactions have  
40 been shown to play an important role in the future summer climate, in particular, over central and southeastern  
41 Europe (Seneviratne et al. 2006, Diffenbaugh 2007, Hirschi et al 2011). In conclusion, the improvements in  
42 the land model incorporated in CM2.5 at its high spatial resolution are responsible for the stark contrast  
43 between the CMIP3/CMIP5 and CM2.5 regional projections (i.e. less intense warming and drying over  
44 Europe, including the minimum of warming and wetting tendencies in southeastern Europe). These feedbacks  
45 should be explored in more detail in future work using targeted experiments like the Global Land-Atmosphere  
46 Coupling Experiment (Seneviratne et al. 2013), but lie outside the scope of this paper.

Monika Barcikowska 8/19/19 11:02 AM  
Formatted [42]

Monika Barcikowska 8/15/19 8:59 AM  
Deleted: .



1 Additionally, we find that the SNAO will have an important role in counterbalancing the thermodynamic  
2 effects of the projected drying over the Mediterranean, simulated in both the CM2.5 and CMIP projections.  
3 We have shown that CM2.5 projects a strengthening of the SNAO towards its positive phase, reflected in the  
4 strengthening of the meridional circulation cells over North Atlantic. The derived changes of the SNAO are  
5 manifest in the positive anomalies of precipitation (wetting) over large parts of the Mediterranean. For  
6 example, without the impact of SNAO, the drying projected in CM2.5 over the Iberian Peninsula, Italy, and  
7 the Balkan coast would be much stronger (locally up to ~30-40%).

8  
9 Nevertheless, our analysis also shows that a) the representation of the regional SNAO impacts, and b) the  
10 projected future evolution of the SNAO is almost the same in CM2.5 and its low-resolution predecessor, i.e.  
11 CM2.1 model, or other previous-generation models. Hence the SNAO teleconnection does not seem to be a  
12 strong candidate for explaining the differences in the future projections for the summer European climate  
13 between CM2.5 and CMIP3/CMIP5 ensembles.

14  
15 Moreover, the future changes in the eastern Mediterranean climate regime projected in CM2.5 suggest a  
16 weakening role of atmospheric dynamics in maintaining the regional hydroclimate and temperature balance.  
17 For example, the projected changes over Asia Minor show very strong drying and warming, despite the  
18 increasing influence (i.e. wetting and cooling) of the SNAO teleconnection. Also, the warming over the Asia  
19 Minor and Levant regions constitutes a local maximum for the warming and drying in the Mediterranean  
20 region, despite the cooling effect of intensifying Etesian winds and the weakening mid- and upper-  
21 tropospheric subsidence in EMED. We found a weakening of the linkage between the low-level circulation  
22 (e.g. northerly flow) and the mid-and upper-level subsidence over the EMED, which are responsible for the  
23 regional temperature balance.

24  
25 This is indicative of the changes in the summer EMED regime introduced by the local surface temperature. By  
26 comparing warmer and cooler EMED seasons in the control run, we found an increasing influence of local  
27 surface temperature on the local low-level atmospheric circulation in a warmer climate. This influence,  
28 consistent with a large sensitivity of the desert-like lands to variations in radiative forcing, is manifest in an  
29 anomalous intensification of the heat low over the EMED, Sahara and the Persian trough, but also in positive  
30 SLP anomalies, increasing subsidence over the central Mediterranean. All of these features are also consistent  
31 with future climate changes projected by CM2.5. This supports the overall notion of the increasing influence  
32 of the warming land surface on the low-level atmospheric circulation, and also a decreasing influence of  
33 teleconnections and local atmospheric dynamics on the future summer climate in this region.

34  
35 Overall, our analysis indicates very profound climate changes for the Mediterranean region in the summer,  
36 although they do not seem to be as radical as projected by the previous generation models. The differences  
37 between CM2.5 projections of future changes and those of previous-generation models points to the role of  
38 factors such as land surface-atmospheric interactions, in particular over central and southeastern Europe,  
39 rather than large-scale atmospheric dynamics and teleconnections. This highlights the importance of the  
40 ability of the future-generation models to capture local land-atmospheric interactions.

41  
42 **"The authors declare that they have no conflict of interest."**

#### 43 **Acknowledgements**

44 The authors are grateful to Ileana Blade, Fred Kucharski and Eduardo Zorita, Salvatore Pascale and Baoqiang  
45 Xiang for helpful comments and discussions.  
46

Monika Barcikowska 8/15/19 8:59 AM

**Deleted:** The CM2.5 projected future circulation over southern Europe also differs from the CMIP ensembles. CM2.5 projections indicate a strengthening of the zonal pressure gradient over the Mediterranean and the associated northerly flow/Etesian winds, contrary to a rather small weakening of the flow projected in CMIP5. This is a direct consequence of a) the strengthening anticyclonic circulation over the North Atlantic and higher sea level pressure over northwestern and central parts of Europe, and b) the intensification of the heat low over Sahara, the Persian trough and Asia Minor. In contrast, the intensified heat low in the CMIP5 ensemble covers not only arid subtropical regions but spreads over most of Eurasia (except the southern part of the monsoon region), suggestive of dominating contributions of land-atmosphere feed... [43]

Monika Barcikowska 8/21/19 7:02 AM

**Formatted:** Font:(Default) Times New Roman

Monika Barcikowska 8/16/19 6:44 AM

**Formatted:** ... [44]

Monika Barcikowska 8/16/19 8:17 AM

**Formatted:** ... [45]

Monika Barcikowska 8/16/19 7:46 AM

**Deleted:** ... weakening role of atm... [46]

Monika Barcikowska 8/16/19 8:17 AM

**Formatted:** Not Highlight

Monika Barcikowska 8/16/19 7:43 AM

**Deleted:** changes...in the Mediterrat... [47]

Monika Barcikowska 8/16/19 8:17 AM

**Formatted:** Not Highlight

Monika Barcikowska 8/16/19 8:15 AM

**Deleted:** - ... [48]

Monika Barcikowska 8/21/19 7:21 AM

**Deleted:** is...indicative of the chang... [49]

Monika Barcikowska 8/23/19 12:15 PM

**Deleted:** - ... [50]

Monika Barcikowska 8/21/19 7:29 AM

**Formatted:** Font:(Default) Times New Roman

1 | **References:**

- 2 Alessandri, A., De Felice, M., Zeng, N., Mariotti, A., Pan, Y., Cherchi, A., Lee, J.Y., Wang, B., Ha, K.J., Ruti,  
3 P., Artale, V.: Robust assessment of the expansion and retreat of Mediterranean climate in the 21st century.  
4 *Sci Rep* 4:7211, 2014  
5  
6 Allan, R. and C.K. Folland, 2018: Atmospheric circulation. 1. Mean sea level pressure and related modes of  
7 variability—In: *State of the Climate 2017. Bull. Amer. Meteor. Soc.*, **99**, S39-S41.  
8  
9 Alpert, P., Osetinsky, I., Ziv, B., Shafir, H.: A new seasons definition based on classified daily synoptic  
10 systems: an example for the eastern Mediterranean. *Int J Climatol* 24:1013–1021, 2004.  
11  
12 Baines, P. and C.K. Folland, 2007: Evidence for a rapid global climate shift across the late 1960s. *J. Climate*,  
13 **20**, 2721-2744.  
14  
15 Barcikowska, M., Knutson, T. and Zhang, R.: Observed and simulated fingerprints of multidecadal climate  
16 variability, and their contributions to periods of global SST stagnation. *Journal of Climate*, 30(2), 2017  
17  
18 Barcikowska, M., Kapnick, S.B., and F. Feser: Impact of large-scale circulation changes in the North Atlantic  
19 sector on the current and future Mediterranean winter hydroclimate. *Climate Dynamics*, 2017b,  
20 doi:10.1007/s00382-017-3735-5  
21  
22 Barnston, A.G., Livezey, R.E.: Classification, seasonality and persistence of low-frequency atmospheric  
23 circulation patterns. *Mon Wea Rev* 115:1083–1126, 1987  
24  
25 Berg, A., B.R. Lintner, K. Findell, S.I. Seneviratne, B. van den Hurk, A. Ducharne, F. Chéruey, S. Hagemann,  
26 D.M. Lawrence, S. Malyshev, A. Meier, and P. Gentine, 2015: Interannual Coupling between Summertime  
27 Surface Temperature and Precipitation over Land: Processes and Implications for Climate Change. *J. Climate*,  
28 28, 1308–1328, <https://doi.org/10.1175/JCLI-D-14-00324.1>  
29  
30 Berg, A., Findell, K., Lintner, B., Giannini, A., Seneviratne, S. I., Van den Hurk, B., Ruth Lorenz, Andy  
31 Pitman, Stefan Hagemann, Arndt Meier, Frédérique Cheruy, Agnès Ducharne, Sergey Malyshev & P. C. D.  
32 Milly, 2016: Land–atmosphere feedbacks amplify aridity increase over land under global warming. *Nature*  
33 *Climate Change*, 6(9), 869.  
34  
35  
36 Blade, I., Liebmann, B., Fortuny, D., van Oldenborgh, G.J.: Observed and simulated impacts of the summer  
37 NAO in Europe: implications for projected drying in the Mediterranean region. *Clim Dyn* 39:709–727, 2012.  
38  
39 Bladé, I., D. Fortuny, van Oldenborgh, G.J., Liebmann, B.: The summer North Atlantic Oscillation in CMIP3  
40 models and related uncertainties in projected summer drying in Europe, *J. Geophys. Res.*, 117, D16104,  
41 2012b  
42  
43 Bitan, A., Saaroni, H.: The horizontal and vertical extension of the Persian Gulf pressure trough. *Int J*  
44 *Climatol* 12:733–747, 1992



1 Booth, B.B.B., Dunstone, N.J., Halloran, P.R., Andrews, T., and N. Bellouin, 2012: Aerosols implicated as a  
2 prime driver of twentieth-century North Atlantic climate variability, *Nature*, **484**, 228–232  
3 doi:10.1038/nature10946

4 Cassou, C., L. Terray, J. W. Hurrell, and C. Deser: North Atlantic winter climate regimes: Spatial asymmetry,  
5 stationarity with time, and oceanic forcing. *J. Climate*, **17**, 1055–1068, 2004  
6

7 Cassou, C., L. Terray, and A. S. Phillips: Tropical Atlantic influence on European heat waves. *J. Climate*, **18**,  
8 2805–2811, 2005  
9

10 Cherchi, A., Annamalai, H., Masina, S., Navarra, A.: South Asian summer monsoon and eastern  
11 Mediterranean climate: the monsoon- desert mechanism in CMIP5 simulations. *J. Clim* **27**: 6877– 6903, 2014  
12

13 [Cherchi, A., Annamalai, H., Masina, S. et al. \*Clim Dyn\* \(2016\) 47: 2361. \[https://doi.org/10.1007/s00382-015-\]\(https://doi.org/10.1007/s00382-015-2968-4\)  
14 \[2968-4\]\(https://doi.org/10.1007/s00382-015-2968-4\)](https://doi.org/10.1007/s00382-015-2968-4)

15 Cheruy, F., J. L. Dufresne, F. Hourdin, and A. Ducharne: Role of clouds and land -atmosphere coupling in  
16 midlatitude continental summer warm biases and climate change amplification in CMIP5 simulations,  
17 *Geophys. Res. Lett.*, **41**, 6493–6500, doi:10.1002/2014GL061145, 2014.  
18

19 Christensen, J. H., and F. Boberg: Temperature dependent climate projection deficiencies in CMIP5 models,  
20 *Geophys. Res. Lett.*, **39**, L24705, doi:10.1029/2012GL053650, 2012.  
21

22 Chronis, T., Raitsos, D.E., Kassis, D., Sarantopoulos, A.: The summer North Atlantic oscillation influence on  
23 the Eastern Mediterranean. *J. Clim* **24**:5584–5596, 2011  
24  
25

26 Collins, M., R. Knutti, J. Arblaster, J.-L. Dufresne, T. Fichet, P. Friedlingstein, X. Gao, W.J. Gutowski, T.  
27 Johns, G. Krinner, M. Shongwe, C. Tebaldi, A.J. Weaver and M. Wehner, 2013: Long-term Climate Change:  
28 Projections, Commitments and Irreversibility. In: *Climate Change 2013: The Physical Science Basis.*  
29 Contribution of Working Group I to the Fifth Assessment Report of the Intergovernmental Panel on Climate  
30 Change [Stocker, T.F., D. Qin, G.-K. Plattner, M. Tignor, S.K. Allen, J. Boschung, A. Nauels, Y. Xia, V. Bex  
31 and P.M. Midgley (eds.)]. Cambridge University Press, Cambridge, United Kingdom and New York, NY,  
32 USA.  
33

34 Compo, G.P., J.S. Whitaker, and P.D. Sardeshmukh, 2006: Feasibility of a 100 year reanalysis using only  
35 surface pressure data. *Bull. Amer. Met. Soc.*, **87**, 175-190, <http://dx.doi.org/10.1175/BAMS-87-2-175>.  
36

37 Compo, G.P., J. S. Whitaker, P. D. Sardeshmukh, N. Matsui, R. J. Allan, X. Yin, B. E. Gleason Jr., R. S. Vose,  
38 G. Rutledge, P. Bessemoulin, S. Brönnimann, M. Brunet, R. I. Crouthamel, A. N. Grant, P. Y. Groisman, P. D.  
39 Jones, M. C. Kruk, A. C. Kruger, G. J. Marshall, M. Maugeri, H. Y. Mok, Ø. Nordli, T. F. Ross, R. M. Trigo,  
40 X. L. Wang, S. D. Woodruff, S. J. Worley, 2011: The twentieth century reanalysis project. *Q. J. R. Meteorol.*  
41 *Soc.* **137**, 1–28.  
42

43 Cornes, R., G. van der Schrier, E.J.M. van den Besselaar, and P.D. Jones. 2018: An Ensemble Version of the  
44 E-OBS Temperature and Precipitation Datasets, *J. Geophys. Res. Atmos.*, **123**. doi:10.1029/2017JD028200  
45

1 Delworth, T.L., A.J. Broccoli, A. Rosati, R.J. Stouffer, V. Balaji, J.A. Beesley, W.F. Cooke, K.W. Dixon, J.  
2 Dunne, K.A. Dunne, J.W. Durachta, K.L. Findell, P. Ginoux, A. Gnanadesikan, C.T. Gordon, S.M. Griffies, R.  
3 Gudgel, M.J. Harrison, I.M. Held, R.S. Hemler, L.W. Horowitz, S.A. Klein, T.R. Knutson, P.J. Kushner, A.R.  
4 Langenhorst, H. Lee, S. Lin, J. Lu, S.L. Malyshev, P.C. Milly, V. Ramaswamy, J. Russell, M.D. Schwarzkopf,  
5 E. Shevliakova, J.J. Sirutis, M.J. Spelman, W.F. Stern, M. Winton, A.T. Wittenberg, B. Wyman, F. Zeng, and  
6 R. Zhang, [GFDL's CM2 Global Coupled Climate Models. Part I: Formulation and Simulation Characteristics](#).  
7 *J. Climate*, 19, 643–674, 2006  
8  
9 Delworth, T.L., A. Rosati, W. Anderson, A.J. Adcroft, V. Balaji, R. Benson, K. Dixon, S.M. Griffies, H. Lee,  
10 R.C. Pacanowski, G.A. Vecchi, A.T. Wittenberg, F. Zeng, and R. Zhang, 2012: [Simulated Climate and](#)  
11 [Climate Change in the GFDL CM2.5 High-Resolution Coupled Climate Model](#). *J. Climate*, 25, 2755–2781,  
12 2012  
13  
14 Delworth, T. and Mann, M.: Observed and simulated multidecadal variability in the Northern Hemisphere  
15 *Climate Dynamics*, 16: 661, 2000  
16  
17 Diffenbaugh, N. S., J. S. Pal, F. Giorgi, and X. Gao: Heat stress intensification in the Mediterranean climate  
18 change hotspot, *Geophys. Res. Lett.*, 34, L11706, doi:10.1029/2007GL030000, 2007  
19  
20 Enfield, D. B., Mestas - Nunez, A.M., Trimble, P.J.: The Atlantic multidecadal oscillation and its relation to  
21 rainfall and river flows in the continental U.S., *Geophys. Res. Lett.*, 28, 2077–2080, 2001  
22  
23 [Fontaine, B. , Roucou, P. , Gaetani, M. and Marteau, R. \(2011\), Recent changes in precipitation, ITCZ](#)  
24 [convection and northern tropical circulation over North Africa \(1979–2007\). \*Int. J. Climatol.\*, 31: 633-648.](#)  
25 [doi:10.1002/joc.2108](#)  
26  
27 Giorgi, F. ; 2006: Climate change hot - spots, *Geophys. Res. Lett.*, 33, L08707, doi:10.1029/2006GL025734.  
28  
29 Giorgi, F. and Lionello, P.: Climate change projections for the Mediterranean region. *Glob Planet Change*  
30 63:90–104, 2008  
31  
32 Feng, S., Hu, Q., Huang, W., Ho, C.-H., Li, R. & Tang, Z. Projected climate regime shift under future global  
33 warming from multi-model, multi-scenario CMIP5 simulations. *Global Planet. Change* 112, 41–52 (2014).  
34 Füssel, H.M., André Jol, Andreas Marx, et al. edited by Hans-Martin Füssel, André Jol, Andreas Marx,  
35 Mikael Hildén: Climate change, impacts and vulnerability in Europe 2016 - An indicator-based report Vol.  
36 1/2017.  
37  
38 Folland, C.K., Knight, J., Linderholm, H.W., Fereday, D., Ineson, S., Hurrell, J.W.: The summer North  
39 Atlantic Oscillation: past, present, and future. *J Climate* 22:1082–1103, 2009  
40  
41 Hanf, F., Körper, J., Spangehl, T. & Cubasch, U. Shifts of climate zones in multi-model climate change  
42 experiments using the Köppen climate classification. *Meteorol. Z.* 21, 111–123 (2012).  
43  
44 Hoskins, B.J.: On the existence and strength of the summer subtropical anticyclones —Bernhard Haurwitz  
45 memorial. *Bull Am Meteorol Soc* 77:1287–1292, 1996  
46

1 HMSO: Weather in the Mediterranean I: general meteorology, 2nd edn. Her Majesty Stationery Office,  
2 London, p 362, 1962  
3  
4 Hurrell, J.W.: Decadal trends in the North Atlantic Oscillation: regional temperatures and precipitation.  
5 *Science* 269:676–679, 1995  
6  
7 Hurrell, J.W., Deser, C.: North Atlantic climate variability: the role of the North Atlantic Oscillation. *J Mar*  
8 *Syst* 78(1): 28–41, 2009  
9  
10 Hurrell, J.W., Folland, C.K.: A change in the summer circulation over the North Atlantic. CLIVAR  
11 Exchanges, No. 25, International CLIVAR Project Office, Southampton, United Kingdom, pp 52–54, 2002  
12  
13 Hurrell, J.W., Kushnir, Y., Ottersen, G., Visbeck, M.: An overview of the North Atlantic Oscillation. *The*  
14 *North Atlantic Oscillation: climatic significance and environmental impact. Geophys Monogr. Am Geophys*  
15 *Union* 134:1–35, 2003  
16  
17 Hurrell, J. W., and H. van Loon: Decadal variations in climate associated with the North Atlantic Oscillation.  
18 *Climatic Change*, 36, 301–326, 1997  
19  
20 Jacob, D., Petersen, J., Eggert, B., Alias, A., Christensen, O. B., Bouwer, L. M., Braun, A., Colette, A., Déqué,  
21 M., Georgievski, G., Georgopoulou, E., Gobiet, A., Menut, L., Nikulin, G., Haensler, A., Hempelmann, N.,  
22 Jones, C., Keuler, K., Kovats, S. et al., 2014, 'EURO-CORDEX: New high-resolution climate change  
23 projections for European impact research', *Regional Environmental Change* 14(2), 563–578 (doi:  
24 10.1007/s10113-013-0499-2).  
25  
26 Kalnay et al., The NCEP/NCAR 40-year reanalysis project, *Bull. Amer. Meteor. Soc.*, 77, 437–470, 1996.  
27  
28 Kanamitsu, M., W. Ebisuzaki, J. Woollen, S. Yang, J.J. Hnilo, M. Fiorino, and G.L. Potter: [NCEP–DOE](#)  
29 [AMIP-II Reanalysis \(R-2\)](#). *Bull. Amer. Meteor. Soc.*, 83, 1631–1644, 2002  
30  
31 Kelley, C., Ting, M., Seager, R., Kushnir, Y.: Mediterranean precipitation climatology, seasonal cycle, and  
32 trend as simulated by CMIP5. *Geophys Res Lett* 39:L21703, 2012  
33  
34 Krichak, S.O., Kishcha, P., Alpert, P.: Decadal trends of main Eurasian oscillations and the Mediterranean  
35 precipitation, *Teor. Appl. Climatol.*, 72: 29–220, 2002  
36  
37 Knight, J. R., R. J. Allan, C. K. Folland, M. Vellinga, and M. E. Mann: A signature of persistent natural  
38 thermohaline circulation cycles in observed climate. *Geophys. Res. Lett.*, 32, L20708, 2005  
39  
40 [Knight, J. R., R. J. Allan, C. K. Folland, and M. E. Mann, 2006: Climatic impacts of the Atlantic multidecadal](#)  
41 [oscillation. \*Geophys. Res. Lett.\*, 33, L17706, doi:10.1029/2006GL026242](#)  
42  
43 Legates, D. R., and C. J. Willmott, 1990: Mean seasonal and spatial variability in gauge-corrected, global  
44 precipitation. *Int. J. Climatol.*, 10, 111–127.  
45

1 Lelieveld, J., Berresheim, H., Borrmann, S., et al.: Global air pollution crossroads over the Mediterranean.  
2 Science 298: 794–799, 2002  
3  
4 Lelieveld, J., Hadjinicolaou, P., Kostopoulou, E., Chenoweth, J., Giannakopoulos, C., Hannides, C., Lange,  
5 M.A., El Maayar, M., Tanarthe, M., Tyrlis, E., Xoplaki, E.: Climate change and impacts in the eastern  
6 Mediterranean and the Middle East. *Clim Chang* 114:667–687, 2012  
7  
8 Lin, H.: Global extratropical response to diabatic heating variability of the Asian summer monsoon. *J Atmos*  
9 *Sci* 66: 2697–2713, 2009  
10  
11 Lin, H., Derome, J., Brunet, G.: The nonlinear transient atmospheric response to tropical forcing. *J Clim*  
12 20:5642–5665, 2007  
13  
14 Linderholm, H.W. and C.K. Folland, 2017: Summer North Atlantic Oscillation (SNAO) variability on  
15 interannual to palaeoclimate time scales. *CLIVAR Exchanges* 72, 57-60 and *Past Global Changes Magazine*,  
16 25, No. 1. doi: 10.22498/pages.25.1.57  
17  
18 Linderholm, H.W., Folland, C.K. and A. Walther, 2009: A multicentury perspective on the summer North  
19 Atlantic Oscillation (SNAO) and drought in the eastern Atlantic Region. *J. Quaternary Science*, 24, 415-425.  
20 Doi:10.1002/jqs.1261  
21  
22 Maheras, P.: Le problem des Etesiens. *Mediterranee*, N40, 57-66, 1980.  
23  
24 Mann, M. E., and Emanuel, K.A.: Atlantic hurricane trends linked to climate change, *Eos Trans. AGU*, 87(24),  
25 233–241, doi: 10.1029/2006EO240001, 2006  
26  
27 Mariotti, A., Dell’Aquila, A.: Decadal climate variability in the Mediterranean region: roles of large-scale  
28 forcings and regional processes. *Clim Dyn* 38:1129–1145, 2012  
29  
30 Mariotti, A., Pan, Y., Zeng, N., Alessandri, A.: Long-term climate change in the Mediterranean region in the  
31 midst of decadal variability. *Clim Dyn* 44:1437–1456, 2015  
32  
33 Mariotti, A., Struglia, M.V., Zeng, N., Lau, K.M.: The hydrological cycle in the Mediterranean region and  
34 implications for the water budget of the Mediterranean Sea. *J Clim* 15:1674–1690, 2002  
35  
36 Meehl, G., A. et al. Global climate projections. In: Solomon S et al. (eds) *Climate change 2007: The Physical*  
37 *Science Basis*. Cambridge University Press, Cambridge, pp 747–845, 2007.  
38  
39 Meinshausen, M. and Smith, J. S and Calvin, K.V. and Daniel, J., and Kainuma, M., and Lamarque, J.-F. and  
40 Matsumoto, K., and A Montzka, S., C B Raper, S., and Riahi, K. and Thomson, A.M. and Velders, Guus J. M.,  
41 and Vuuren, D: The RCP greenhouse gas concentrations and their extensions from 1765 to 2300. *Climatic*  
42 *Change*, 2011  
43  
44 Metaxas D.A: The interannual variability of the Etesian frequency as a response of atmospheric circulation  
45 anomalies. *Bulletin of the Hellenic Meteorological Society* 2(5): 30–40, 1977  
46

1 Milly, P.C., S.L. Malyshev, E. Shevliakova, K.A. Dunne, K.L. Findell, T. Gleeson, Z. Liang, P. Phillipps, R.J.  
2 Stouffer, and S. Swenson, 2014: An Enhanced Model of Land Water and Energy for Global Hydrologic and  
3 Earth-System Studies. *J. Hydrometeor.*, 15, 1739–1761, <https://doi.org/10.1175/JHM-D-13-0162.1>  
4  
5 Mueller, B., and S. I. Seneviratne (2014), Systematic land climate and evapotranspiration biases in CMIP5  
6 simulations, *Geophys. Res. Lett.*, 41, 128–134, doi:10.1002/2013GL058055, 2014.  
7  
8 Mueller, B., and S. I. Seneviratne (2012), Hot days induced by precipitation deficits at the global scale, *Proc.*  
9 *Natl. Acad. Sci. U. S. A.*, 109, 12,398–12,403, doi:10.1073/pnas.1204330109, 2012.  
10  
11 Prezerakos, N.G.: Does the extension of the Azores anticyclone towards the Balkans really exist. *Archive fur*  
12 *Meteorologie, Geophysik und Bioklimatologie, Serie A: Meteorologie und Geophysik* 33: 217–227, 1984  
13  
14 Poli, P., H. Hersbach, P. Berrisford, and coauthors: ERA-20C Deterministic. ERA Report Series Number 20,  
15 2015  
16  
17 Riahi, K., Rao, S., Krey, V. et al. *Climatic Change*, 109: 33. 2011  
18  
19 Raicich, F., Pinardi, N., Navarra, A.: Teleconnections between Indian monsoon and Sahel rainfall and the  
20 Mediterranean. *Int J Climatol* 23:173–186, 2003  
21  
22 Rizou, D., Flocas, H.A., Athanasiadis, P., Bartzokas, A.: Relationship between the Indian summer monsoon  
23 and the large-scale circulation variability over the Mediterranean, *Atmospheric Research*, Volume 152, 159-  
24 169, 2015.  
25  
26 Reddaway, J.M., Bigg, G.R.: Climatic change over the Mediterranean and links to the more general  
27 atmospheric circulation. *Int J Climatol* 16:651–661, 1996  
28  
29 Rodwell, M.J., Hoskins, B.J.: Monsoons and the dynamics of deserts. *Q J R Meteorol Soc* 122:1385–1404,  
30 1996  
31  
32 Rodwell, M.J., Hoskins, B.J.: Subtropical anticyclones and summer monsoons. *J Clim* 14:3192–3211, 2001  
33  
34 Rotstayn, L., and U. Lohman: Tropical rainfall trends and the indirect aerosol effect. *J. Climate*, 15, 2103–  
35 2116, 2002  
36  
37 [Rowell, D.P., 2003: The Impact of Mediterranean SSTs on the Sahelian Rainfall Season. J. Climate, 16, 849–](https://doi.org/10.1175/1520-0442(2003)016<0849:TIOMSO>2.0.CO;2)  
38 [862, https://doi.org/10.1175/1520-0442\(2003\)016<0849:TIOMSO>2.0.CO;2](https://doi.org/10.1175/1520-0442(2003)016<0849:TIOMSO>2.0.CO;2)  
39  
40 Rowell, D.P. and Jones, R.G., 2006: [Causes and uncertainty of future summer drying over Europe](#). *Climate*  
41 *Dynamics*, 27: 281-299  
42  
43 Saaroni, H., Ziv, B.: Summer rain episodes in a Mediterranean climate, the case of Israel: climatological-  
44 dynamical analysis. *Int J Climatol* 20:191–209, 2000  
45

1 Saaroni, H., Ziv, B., Osetinsky, I., Alpert, P.: Factors governing the interannual variation and the long-term  
2 trend of the 850 hPa temperature over Israel. *Q J R Meteorol Soc* 136:305–318, 2010  
3  
4 Scaife, A., Folland, C.K., Alexander, L.V. Moberg, A., Brown, S. and J.R. Knight, 2008: European climate  
5 extremes and the North Atlantic Oscillation. *J. Climate*, **21**, 72-83.  
6  
7 Seneviratne, S. I., D. Lüthi, M. Litschi, and C. Schär: Land atmosphere coupling and climate change in  
8 Europe, *Nature*, 443(7108), 205–209, doi:10.1038/nature05095, 2006  
9  
10 Seneviratne, S. I., et al. : Changes in climate extremes and their impacts on the natural physical environment,  
11 in *Managing the Risks of Extreme Events and Disasters to Advance Climate Change Adaptation. A Special*  
12 *Report of Working Groups I and II of the Intergovernmental Panel on Climate Change (IPCC)*, edited by C. B.  
13 Field et al., pp. 109–230, Cambridge Univ. Press, Cambridge, U. K, 2012  
14  
15 Sutton, R. T., and D. L. R. Hodson: Atlantic Ocean forcing of the North American and European summer  
16 climate. *Science*, 309, 115–118, 2005  
17  
18 Trenberth K.E., Paolino D.A. Jr: The Northern Hemisphere sea level pressure data set: trends, errors and  
19 discontinuities. *Mon Wea Rev*, 108:855–872, 1980  
20  
21 Tyrllis, E., Lelieveld, J., Steil, B.: The summer circulation over the Eastern Mediterranean and the Middle  
22 East: influence of the South Asian monsoon. *Clim Dyn* 40:1103–1123, 2013  
23  
24 Willmott, C. J. and K. Matsuura: *Terrestrial Air Temperature and Precipitation: Monthly and Annual Time*  
25 *Series (1950 - 1999)*, 2001  
26  
27 Zecchetto, S., de Biasio, F.: Sea surface winds over the Mediterranean basin from satellite data (2000-04):  
28 meso- and local-scale features on annual and seasonal time scales. *J Appl Meteorol Climatol* 46:814–827,  
29 2007  
30  
31 Ziv, B., Saaroni, H., Alpert, P.: The factors governing the summer regime of the eastern Mediterranean. *Int J*  
32 *Climatol* 24:1859–1871, 2004  
33  
34  
35  
36  
37  
38  
39  
40  
41  
42  
43  
44  
45  
46



1 Table1 Abbreviation names for the CM2.5 experiments

2

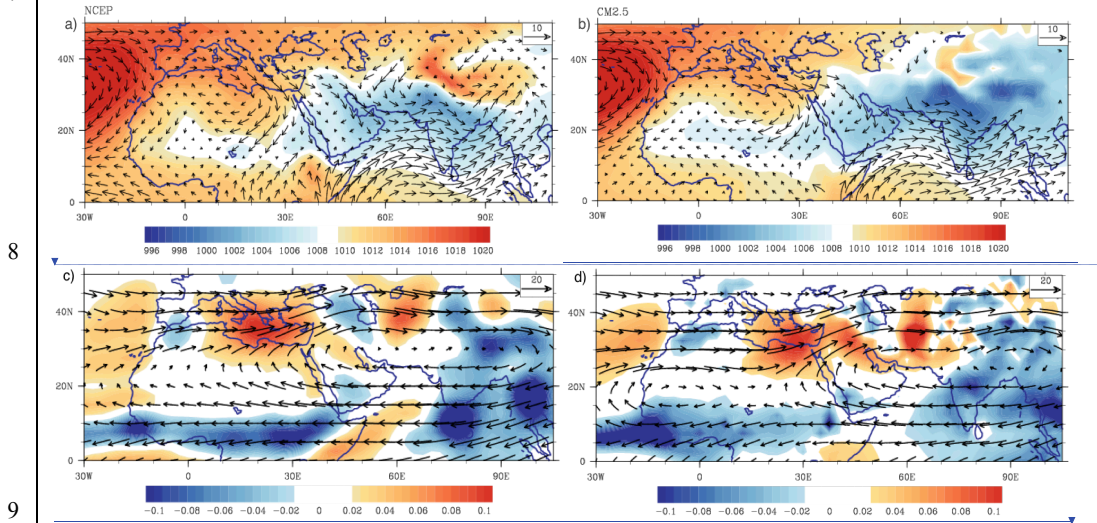
NAME of the experiment	Ensemble size	Number of years total	Historical period [yrs]
<u>CTRL</u>	1	1000 yrs	-
HIST	5	145	1861-2005
<u>PROJ</u>	5	95	2006-2100

3  
4  
5  
6  
7  
8  
9  
10  
11  
12  
13  
14  
15  
16  
17  
18  
19  
20  
21  
22  
23  
24  
25  
26  
27  
28  
29  
30  
31  
32  
33  
34  
35  
36  
37  
38  
39  
40

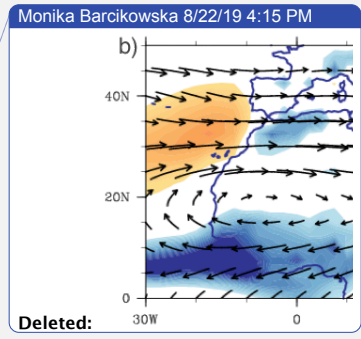
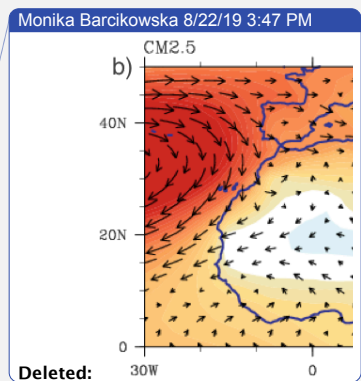
Monika Barcikowska 8/23/19 5:55 AM  
Deleted: - [52]

1 | FIGURES

2  
3 | Figure 1. Seasonal (JJA) time-mean sea level pressure (hPa) and wind vector at 850hPa (m/s) in a) NCEP-DOE2,  
4 | b) CM2.5. Seasonal (July) time-mean vertical velocities at 500hPa (Pa/s) and wind vectors at 200hPa (Pa/s),  
5 | estimated for c) NCEP-DOE2, and d) CM2.5 CTRL. Observational data is used for 1979-2017, control  
6 | simulations data is used for years 101-1000. All data sets are interpolated to the 2.5° horizontal grid.

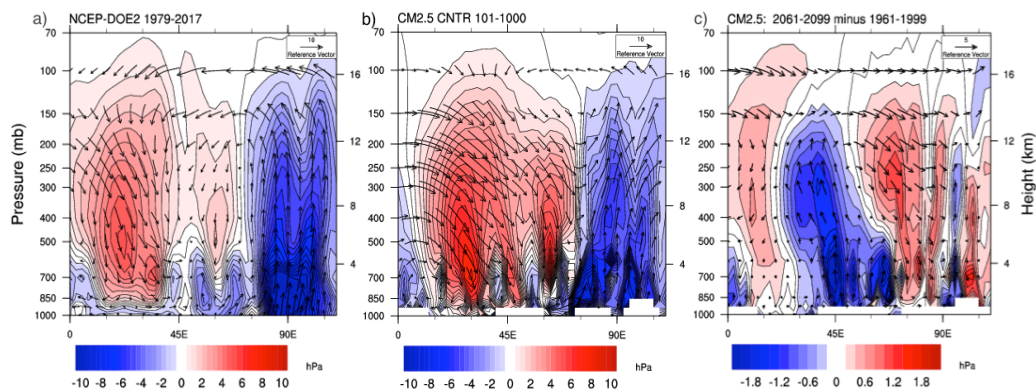


Monika Barcikowska 8/22/19 4:13 PM  
Deleted:  
Monika Barcikowska 8/22/19 4:14 PM  
Deleted: from  
Monika Barcikowska 8/22/19 4:15 PM  
Deleted:  
Monika Barcikowska 8/22/19 4:15 PM  
Deleted: of the control simulations are used, and years 1979-2017 of the observed data.  
Monika Barcikowska 8/22/19 3:49 PM  
Deleted: ... [53]



1 | **Figure 2. Height (pressure)-longitude cross-section of vertical velocity (Pa/s, shaded contours, downward motion**  
 2 **denoted with positive values) and vector of zonal wind (m/s) and vertical velocity (converted to m/s and scaled**  
 3 **with a factor of 1000) in July. Figure shows time-mean values in July a) derived for the period 1979-2017 in**  
 4 **NCEP-DOE2, b) derived from 101-1000 years of CNTL run in CM2.5; and c) projected future changes in the**  
 5 **period 2061-2099 in PROJ ensemble mean, compared with the baseline period 1961-1999 in the HIST ensemble**  
 6 **mean. All fields are shown on the 2.5°x2.5° horizontal grid and at the original vertical levels, common for CM2.5**  
 7 **and NCEP-DOE2.**

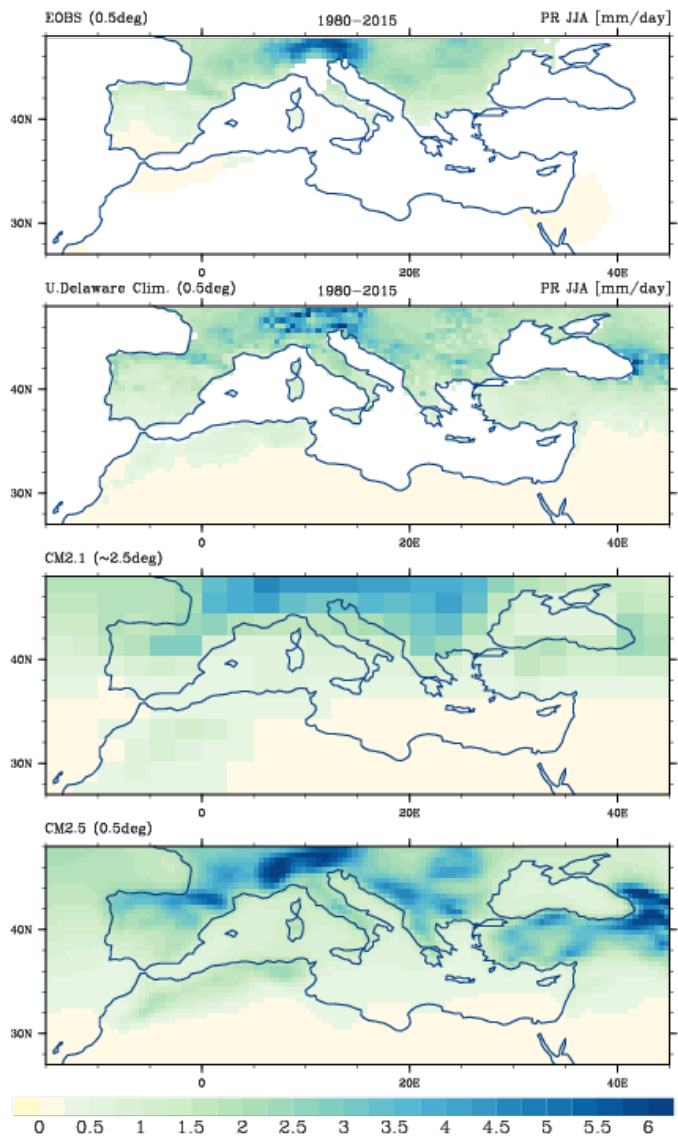
Monika Barcikowska 8/23/19 5:55 AM  
 Deleted: - ... (54)  
 Monika Barcikowska 8/23/19 5:56 AM  
 Deleted: 3



9  
10  
11  
12  
13  
14  
15  
16  
17  
18  
19  
20  
21  
22  
23  
24  
25  
26  
27  
28  
29  
30  
31  
32  
33  
34

1 | Figure 3. Seasonal (JJA) mean precipitation (mm/day) for a) EOBS observations, b) University of Delaware  
2 | Climatology, b) CM2.1, c) CM2.5. The time-mean of seasonal data from years 101–1000 of the control  
3 | simulations are used, and years 1980–2015 of the observed data sets. Both observational data sets are shown at  
4 | 0.5° lat x lon resolution. Regions with missing data are left blank.  
5

Monika Barcikowska 8/23/19 5:56 AM  
Deleted: 4



6

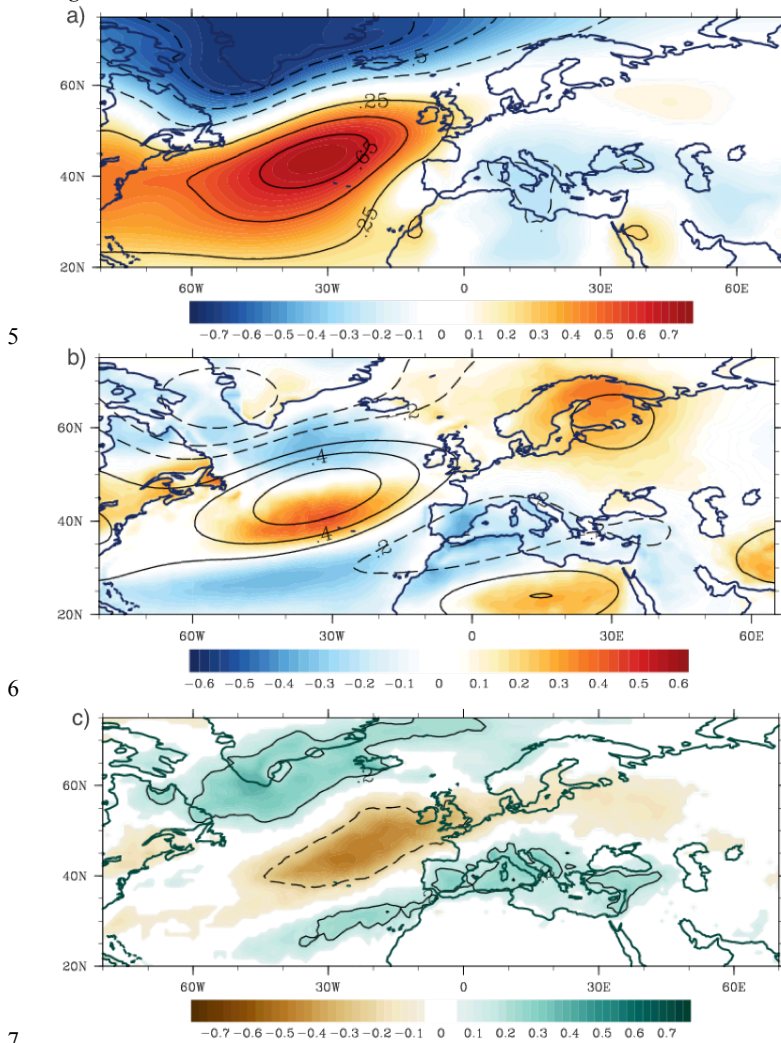
1 | **Figure 4.** Correlation between principal component time series of the SNAO SLP in JA and a) sea level pressure  
2 | b) temperature at 2m (shaded) and geopotential height at 850hPa (contours), c) precipitation. All derived from  
3 | the CTRL run. Contours in a) and c) are shown for 0.25 and 0.5 correlations. Correlations are shown only when  
4 | significant at 1% level.

Monika Barcikowska 8/23/19 5:56 AM

Deleted: -

Monika Barcikowska 8/23/19 5:56 AM

Deleted: 5



7  
8  
9  
10  
11

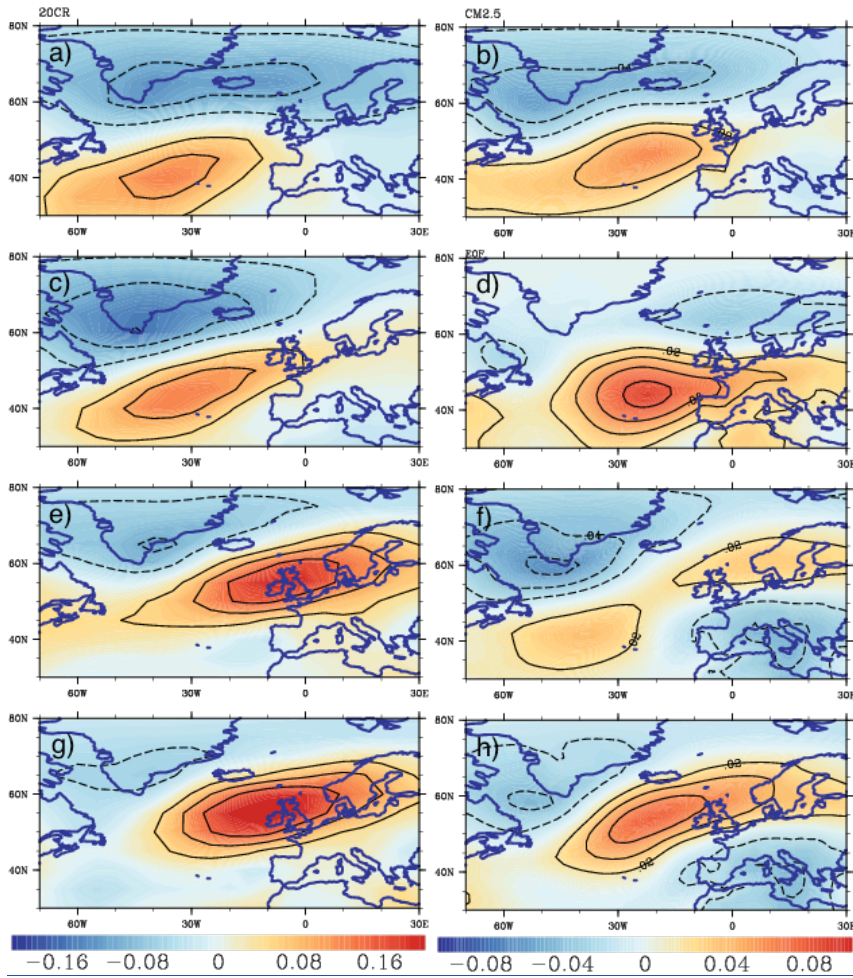
1 | **Figure 5.** Spatial pattern of the SNAO (EOF), derived from the 20CR reanalysis (left), and from the first CM2.5  
 2 | HIST run (right), shown as correlations between the first principal component time series and SLP in July-  
 3 | August. The pattern is derived from periods a)-b) 1870-1920, c)-d) 1900-1950, e)-f) 1940-1990, g)-h) 1960-2010.  
 4 | Please note that the sign of each derived EOF is arbitrary. The analysis took into account that fact and unified the sign,  
 5 | showing the SNAO at its positive phase.  
 6 |

Monika Barcikowska 8/23/19 5:56 AM

Deleted: -

Monika Barcikowska 8/23/19 5:56 AM

Deleted: 6



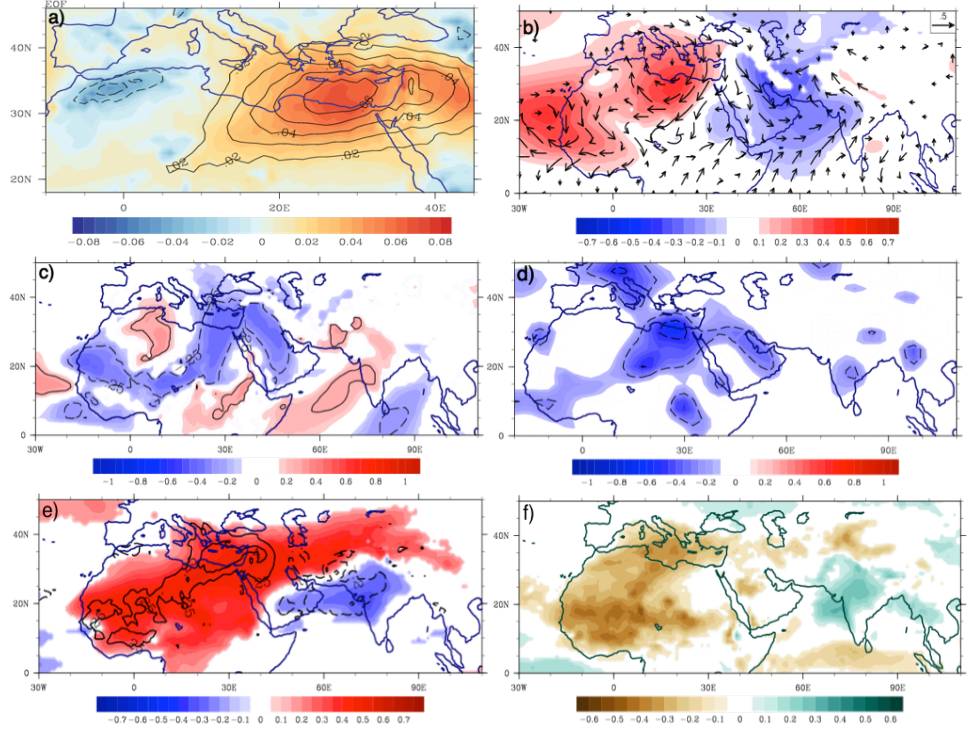
7  
8  
9  
10  
11  
12



1  
2  
3  
4  
5  
6  
7  
8  
9

Figure 6, a) First EOF of the vertical velocity at 500 hPa (EOF1 omega, shaded) and at 300hPa (contours), derived for each level separately and from the monthly mean of July in the CTRL run. The time series of EOF1 omega at 500 hpa are correlated with b) geopotential height (shaded), u, v components (shown as vector) at 850hPa, c) meridional wind at 850hPa, e) outgoing long wave radiation (shaded), omega at 500 hPa (contours: -0.2, 0.2, 0.4), f) precipitation, d) Correlations derived between the observed (NCEP) omega 500hPa over the eastern Mediterranean region (32°-34°N, 25°-30°E) and the meridional wind at 850hPa. Correlations shown for b), c), e), f) at the 1%, and for d) the 10% significance level.

10  
11



12  
13  
14  
15  
16  
17  
18  
19  
20  
21  
22  
23

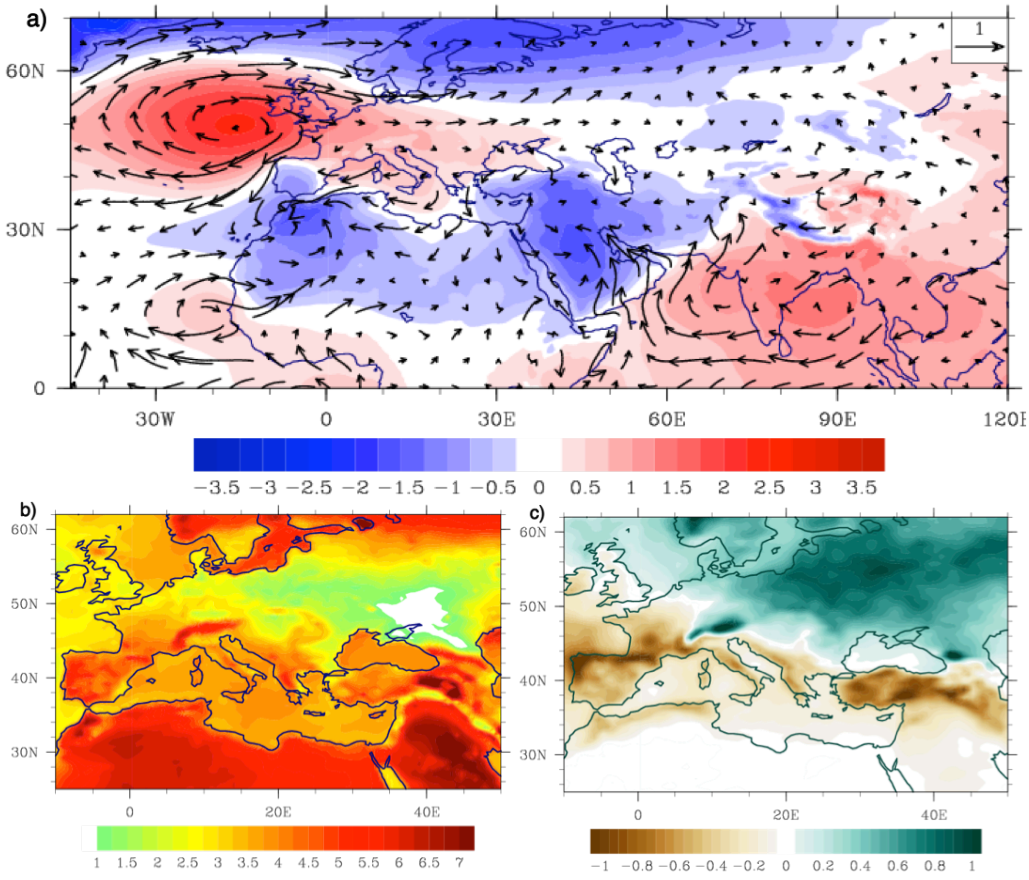
- Monika Barcikowska 8/22/19 3:42 PM
- Deleted: -
- Monika Barcikowska 8/23/19 5:57 AM
- Deleted: 7
- Monika Barcikowska 8/23/19 9:57 AM
- Deleted: of CM2.5 vertical velocities
- Monika Barcikowska 8/23/19 9:57 AM
- Deleted: d
- Monika Barcikowska 8/23/19 6:15 AM
- Deleted:
- Monika Barcikowska 8/23/19 10:02 AM
- Deleted:
- Monika Barcikowska 8/22/19 3:41 PM
- Deleted: and
- Monika Barcikowska 8/22/19 3:41 PM
- Deleted: .
- Monika Barcikowska 8/22/19 3:40 PM
- Deleted: are at
- Monika Barcikowska 8/22/19 3:40 PM
- Deleted: -
- Monika Barcikowska 8/22/19 3:42 PM
- Deleted:

1  
2  
3  
4  
5  
6

Figure 7. Projected future changes for the summer (JJA) a) sea level pressure (hPa, shaded) and u,v wind components at 850hPa (m/s, vector), b) surface temperature (°C), c) total precipitation rate [mm/day], over the period 2061-2099 compared with the baseline period 1961-1999. Changes are derived at the original horizontal resolution.

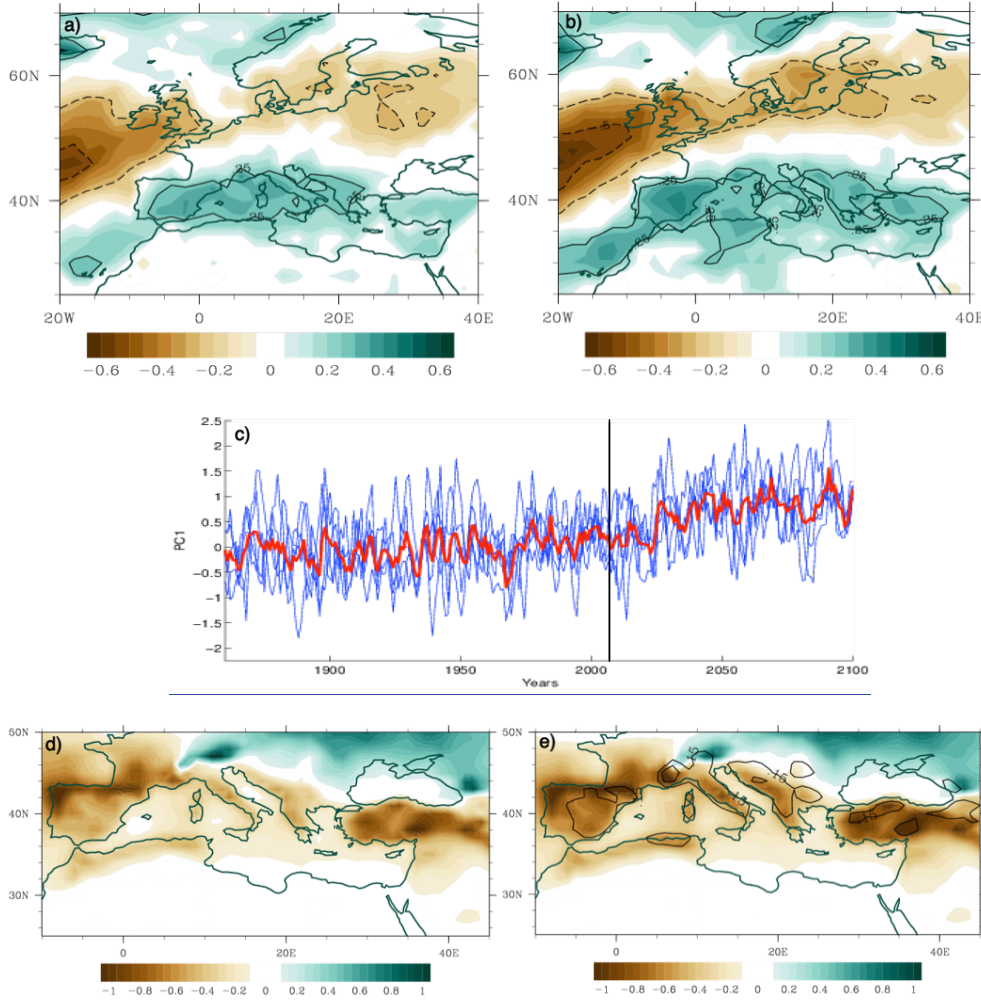
Monika Barcikowska 8/23/19 6:15 AM  
Deleted: 9

7

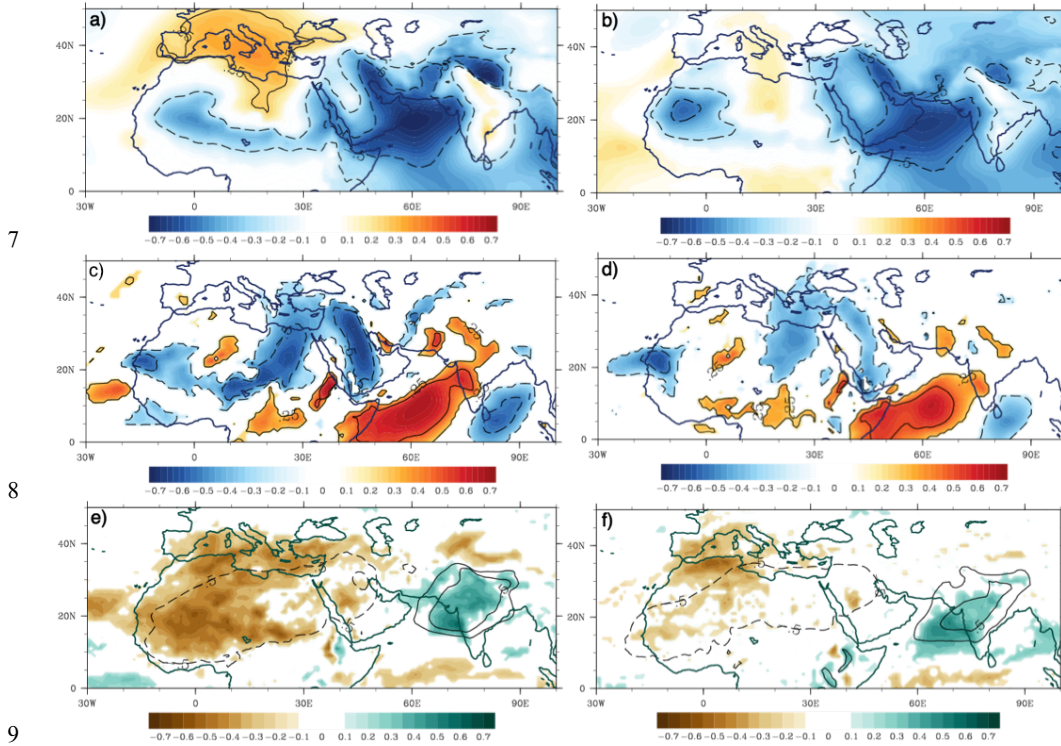


8  
9  
10  
11  
12  
13  
14  
15  
16  
17

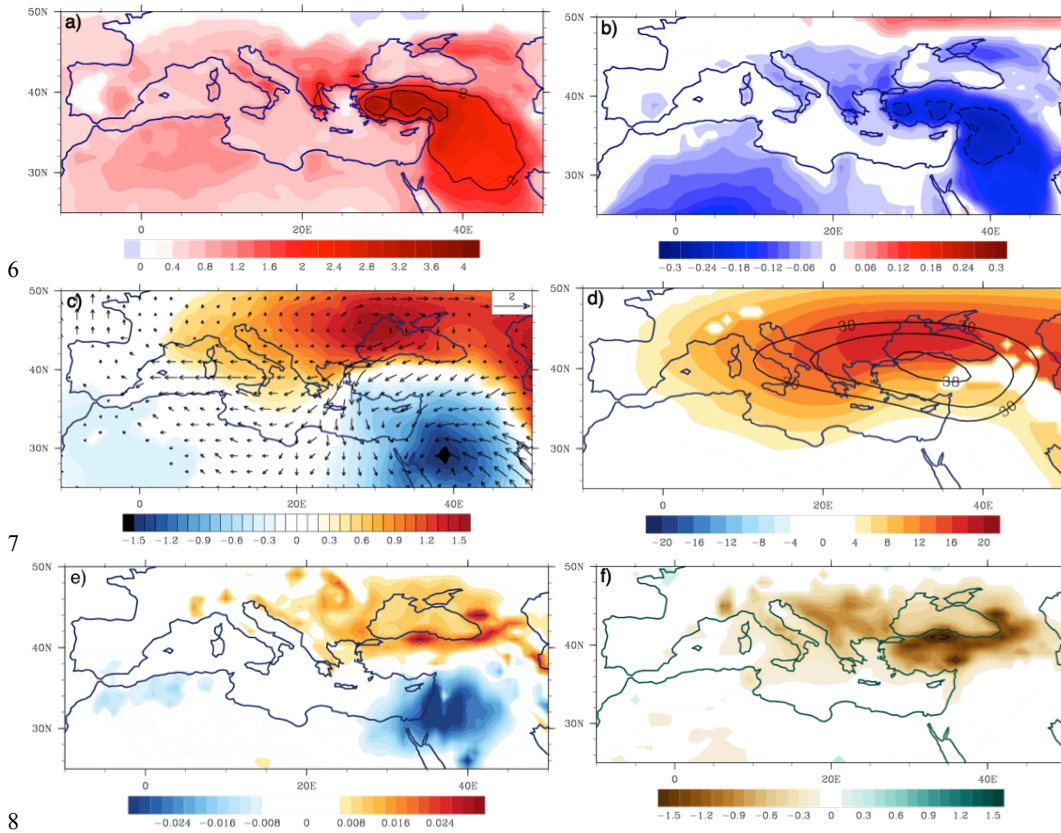
1  
2 **Figure 8.** (a, b) Correlations (shaded) between the SNAO time series and precipitation in 1900-1950 (a) HIST  
3 runs), and 2050-2100 (b) PROJ runs). Contours denote 0.25 and 0.5. c) Evolution of SNAO SLP time series in  
4 1850-2100 period for each run (blue) and the ensemble mean (red). The vertical line divides the HIST and PROJ  
5 time series. (d, e) Projected future changes in the summer precipitation (mm/day) (as in Fig 8c, except that  
6 estimated at 1° horizontal resolution), d) including SNAO impact and e) with the impact of the future SNAO  
7 removed (shaded). The impact of SNAO is estimated based on the linear regression between the detrended time  
8 series of SNAO and precipitation.



1 | Figure 9. Correlations between the PC1 time series of omega at 500hPa in July and surface atmospheric  
2 | circulation in the periods (a,c,e) 1960-2010 and (b,d,f) 2050-2100. Correlation values are estimated for a)-b) SLP  
3 | (shaded and contours), c)-d) meridional wind (shaded and contours), e)-f) precipitation (shaded and contours)  
4 | and vertically integrated water vapor (contours for the values -0.5, 0.3, 0.5). For a)-d) contours are shown for  
5 | 0.25 and 0.5 correlation values.  
6



1 | **Figure 10, a) Composite differences between the sample with the 300 warmest and 300 coolest seasons over the**  
 2 **eastern Mediterranean (30°-36°N, 36°-42°E), for July in the CTRL run, derived from a) surface temperature**  
 3 **(°C), and associated differences in b) relative humidity, c) SLP (hPa) and vector wind at 850hpa (m/s), d) height**  
 4 **at 850hPa (shaded) and 500hPa (contours), e) omega at 500 hPa, f) precipitation (mm/day).**



Monika Barcikowska 8/23/19 6:15 AM

Deleted: -

Monika Barcikowska 8/23/19 6:15 AM

Deleted: 2



1  
2 **Supplementary Material**

3  
4 Fig SI1. Spatial pattern of SNAO, derived from the 20CR reanalysis, derived from periods: 1851-1890, 1891-1930, 1931-1970, 1971-2010.

5  
6  
7 Fig SI2. Spatial patterns of the SNAO using SLP, derived from five HIST runs in 1870-1920 (left column), and 1960-2010 (right column). The pattern is shown as correlations between time series of the first PC of SLP and SLP fields in July-August. The sign of each derived EOF is arbitrary, but here the signs were converted to match the SNAO at its negative phase.

8  
9  
10  
11  
12 Fig SI3. Spatial pattern of SNAO using SLP derived from the period 1970-2030 in the five HIST+PROJ runs. The pattern is shown as correlations between the principal component time series of the first EOF of SLP and SLP fields in July-August.

13  
14  
15  
16 | Fig SI4. Future changes projected for vertical velocities at a) 500 hPa, c) 600 hPa, e) 700 hPa in JJA and in July in b), d), f) respectively. The changes are derived in the period 2061-2099 and compared with the baseline period 1961-1999, derived at the original horizontal resolution (~0.25°). The vertical axis is oriented downward, i.e. negative tendencies (in blue) indicate upward motion while positive tendencies (red, stronger subsidence) indicate downward motion.

17  
18  
19  
20  
21  
22 | Figure SI5. Projected future changes for the summer (JJA) surface temperature (left, °C), and precipitation (right, mm/day) based on the 10-member ensemble simulations of the CSIRO-Mk3-6-0 model, for the forcing scenario RCP8.5.

23  
24  
25  
26 | Fig SI6. As in Fig 9, except that correlations are derived, based on the sample with the 300 coldest (a,b) and 300 warmest (c,d) complete seasons over the eastern Mediterranean in the CTRL run. Correlations are shown for a)-b) meridional wind, c)-d) precipitation.

27  
28  
29  
30 | Fig SI7. As in Fig 10c, except that for a) June, b) August, and for a larger domain.

31  
32 | Fig SI8. As in Fig 10c, except that the regions used for differentiation between warmest and coolest seasons are larger: a) 0°-40°E, 30°-36°N, b) 20°-40°E, 30°-36°N, c) 30°-50°E, 30°-36°N, d) 30°-50°E, 30°-40°N, e) 30°-50°E, 30°-45°N.

33  
34  
35  
36 | Fig SI9. Correlations between the principal component time series of EOF1 omega over EMED and precipitation in (a) June, (b) July (as in Figure 6f), (c) August. Solid lines denote positive correlations, and stippled denote negative correlations, both for the absolute values larger, than 0.25.

Monika Barcikowska 8/23/19 6:49 AM  
Deleted: 5

Monika Barcikowska 8/23/19 6:50 AM  
Deleted: 6

Monika Barcikowska 8/23/19 6:50 AM  
Deleted: 7

Monika Barcikowska 8/23/19 6:50 AM  
Deleted: 11

Monika Barcikowska 8/23/19 6:50 AM  
Deleted: 8

Monika Barcikowska 8/23/19 6:50 AM  
Deleted: ure

Monika Barcikowska 8/23/19 6:50 AM  
Deleted: 2

Monika Barcikowska 8/23/19 6:50 AM  
Deleted: 9

Monika Barcikowska 8/23/19 6:50 AM  
Deleted: ure

Monika Barcikowska 8/23/19 6:50 AM  
Deleted: 2

Monika Barcikowska 8/23/19 6:50 AM  
Deleted: 10

Monika Barcikowska 8/23/19 6:50 AM  
Deleted: 8c